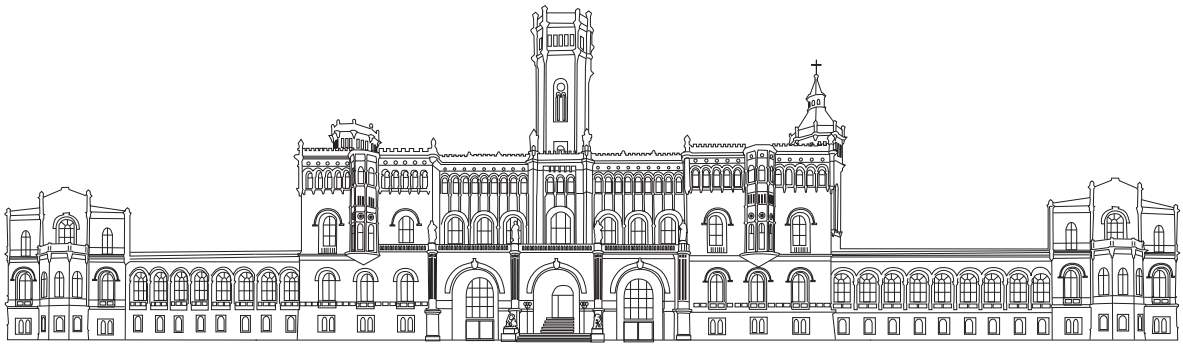

Leibniz Universität Hannover

Fakultät für Mathematik und Physik

Institut für Theoretische Physik

Generation of Electromagnetic Knot Solutions in Minkowski Space

Master‘s Thesis

Submitted by

Colin Kai-Uwe Becker

23.01.2020

First Examiner/Supervisor: Prof. Dr. Olaf Lechtenfeld

Second Examiner: Prof. Dr. Holger Frahm

Ehrenwörtliche Erklärung

Hiermit erkläre ich, dass ich die vorliegende Masterarbeit selbstständig ohne Hilfe Dritter und nur mit den angegebenen Quellen und Hilfsmitteln angefertigt habe. Alle Ausführungen, die wörtlich oder inhaltlich aus den Quellen entnommen wurden, habe ich als solche kenntlich gemacht.

Diese Arbeit hat in gleicher oder ähnlicher Form noch keiner Prüfungsbehörde vorgelegen.

Hannover, den 23.01.2020

Colin Becker

Contents

Notation and Conventions

Throughout this thesis the Einstein summation convention is used. In some places the summation is written in complete form for the sake of introducing new summation indices. Calligraphically written symbols always describe quantities in de Sitter space and will never occur with arrows denoting a vector valued quantity. In the shown visualizations of the field lines for different solutions, the electric field lines will always be colored in green and the magnetic ones in red. Groups are being displayed in capital letters unlike their corresponding algebras that are written in small letters (e.g $SU(2)$ and $su(2)$). Below a legend of frequently used symbols and quantities is listed:

$F, \mathcal{F}$: Electromagnetic field strength tensor

$A, \mathcal{A}$: Electromagnetic gauge potential

$F_D, \mathcal{F}_D, A_D, \mathcal{A}_D$: Dual field strength tensor and gauge potential

$\vec{E}, \mathcal{E}, \vec{B}, \mathcal{B}$: Electric and magnetic fields

$\vec{\mathrm{F}}, \mathrm{F}$: Riemann-Silberstein vector

$\star$: Hodge star operator

$X_{[a}Y_{b]}$: commutation of indices $X_aY_b - X_bY_a$

$[z_1 : z_2 : \cdots : z_n]$: projective coordinates

$\dot{X}(\tau, \omega), \ddot{X}(\tau, \omega)$: The notation of dots as symbols for total time derivatives are expanded to partial derivatives with respect to the cylinder time variable ∂_τ and ∂_τ^2 on de Sitter space

Abstract

In this master thesis, a new way of constructing electromagnetic knot solutions based on [1] is reviewed and expanded on the formalism of working with general superpositions of electromagnetic field configurations for fixed spin. From this formalism, a general relation between energy and helicity is derived and a detailed analysis of such general field configurations satisfying the null field condition is given. It turns out, that these conditions can be brought into connection to a set of geometric interesting equations in $\mathbb{CP}^3$. In addition to that, some field line configurations for numerous solutions arising from this construction method are being visualized and their behaviour during time evolution is shown, if possible in terms of numerical accuracy.

1 Introduction

In this introductory chapter, brief insights into the research area of electromagnetic knots will be given and some important formalism and quantities that are necessary for this thesis will be defined. Furthermore, the conformal equivalence of 4-dimensional de Sitter space to a real finite cylinder over a 3-sphere and half of Minkowski space is described which constitutes the foundation for the method of constructing electromagnetic knot solutions in Minkowski space. Basic knowledge about electrodynamics, differential geometry and Lie groups is assumed.

1.1 Electromagnetic knots

Throughout this whole thesis, we will work with source-free electromagnetic fields that are solutions of the vacuum Maxwell's equations

$$\mathrm{d}F = \mathrm{d} \star F = 0. \tag{1.1}$$

The main focus lies on some special kinds of electromagnetic fields with a non-trivial topology in their electric- and magnetic field line configuration. Such fields with linked field lines are referred to as electromagnetic knots. Publications about electromagnetic knots go back as far as the late 1980's [2] and this topic is still an active field of research [3], [4], [5], [6]. In a great scientific review providing a detailed overview about electromagnetic knots [7], amongst treating some further perspectives about quantized fields and experimental realization, the authors present four known ways of generating electromagnetic knot solutions and discuss them in detail. Those are the so called Rañada formalism and Batemans construction as well as one method based on twistor formalism and another method based on conformal inversions. Mathematically, they are very different from each other and were developed independently but they are of course closely related in terms of their physical meaning. A new construction method that again mathematically highly differs from the previous ones, was recently published in [1] and leaves much room to rediscover known solutions and to possibly obtain completely new insights in this area of research, what motivated the work done in this thesis.

To describe how knotted or linked a field is, one commonly uses an average measure for its electric and magnetic field lines

$$h_m = \frac{1}{2}\int_{\mathbb{R}^3}(A \wedge F) \quad \text{and} \quad h_e = \frac{1}{2}\int_{\mathbb{R}^3}(A_D \wedge F_D), \tag{1.2}$$

called the magnetic helicity h_m and electric helicity h_e. This concept is used for a variety of phenomena, for example in astro- and solar physics to describe solar eruptivity [8] [9] or in fluid dynamics (a short overview about several phenomena can be seen in [10]). In general, h_m and h_e are not constant during time evolution, due to (cf. [7] p.19)

$$\dot{h}_e \propto \int_{\mathbb{R}^3} \vec{E} \cdot \vec{B}\ \mathrm{d}^3x, \tag{1.3}$$

$$\dot{h}_m \propto -\int_{\mathbb{R}^3} \vec{E} \cdot \vec{B}\ \mathrm{d}^3x. \tag{1.4}$$

One often uses the combined electromagnetic helicity $h_{em} = h_e + h_m$ as an average measure for the fields topology and as can clearly be seen from (1.3) and (1.4), h_{em} is constant at all times. The following explanations are based on [11].

Conservation of electric and magnetic helicity can be interpreted as conservation of the topological structure of the field lines on average without giving information about the topology of each individual field line. A special case, where the evolution of each individual field line can be expressed in a remarkably simple way is given for so called null fields, satisfying

$$F_{ab}F^{ab} = F_{ab}(\star F)^{ab} = 0, \tag{1.5}$$

what corresponds to

$$\vec{E} \cdot \vec{B} = 0 \quad \text{and} \quad \vec{E} \cdot \vec{E} - \vec{B} \cdot \vec{B} = 0. \tag{1.6}$$

It is common to express electromagnetic fields as Riemann-Silberstein vectors

$$\vec{F} = \vec{E} + \mathrm{i}\vec{B}, \tag{1.7}$$

so the null condition can be compactly written as

$$\vec{F} \cdot \vec{F} = 0. \tag{1.8}$$

These fields evolve by smooth deformation of their field lines that can be described as a transportation via a velocity field

$$\vec{\nu} = \frac{\vec{E} \times \vec{B}}{\vec{B} \cdot \vec{B}}. \tag{1.9}$$

For this to be true, the so called frozen field condition

$$[\vec{B}, \vec{\nu}] - \dot{\vec{B}} = 0 \quad \text{or equivalently} \quad \nabla \times (\vec{\nu} \times \vec{B}) - \dot{\vec{B}} = 0 \tag{1.10}$$

has to be satisfied. Substituting (1.9) into (1.10) and using the vector formulation of Maxwell‘s equations, it follows that

$$\begin{aligned} \nabla \times (\frac{\vec{E} \times \vec{B}}{\vec{B} \cdot \vec{B}} \times \vec{B}) - \dot{\vec{B}} &= \nabla \times (-(\vec{E} \cdot (\frac{\vec{B} \cdot \vec{B}}{\vec{B} \cdot \vec{B}}) - \vec{B} \cdot (\frac{\vec{E} \cdot \vec{B}}{\vec{B} \cdot \vec{B}}))) - \dot{\vec{B}} \\ &= \nabla \times (\vec{B} \cdot (\frac{\vec{E} \cdot \vec{B}}{\vec{B} \cdot \vec{B}})) = 0. \end{aligned} \tag{1.11}$$

Hence the frozen field condition is only satisfied for $\vec{E} \cdot \vec{B} = 0$, which generally holds for null fields. It is possible for some non-null electromagnetic field to satisfy $\vec{E} \cdot \vec{B} = 0$ at a specific time though. From (1.3) and (1.4) the special property that h_e and h_m are constant individually at any time for null fields can be observed. Because the helicities are closely related to the Gauss‘ linking number of the field lines [cf. [7] Appendix A], this results in an invariant linking number of electric and magnetic field lines during

time evolution.

One famous solution of this kind is the so called Hopf-Rañada knot that can be represented via the following Riemann-Silberstein vector

$$\vec{F}_{HR} = \frac{1}{((t-\mathrm{i})^2 - r^2)^3} \begin{pmatrix} (x-\mathrm{i}y)^2 - (t-\mathrm{i}-z)^2 \\ \mathrm{i}(x-\mathrm{i}y)^2 + \mathrm{i}(t-\mathrm{i}-z)^2 \\ -2(x-\mathrm{i}y)(t-\mathrm{i}-z) \end{pmatrix}. \tag{1.12}$$

Its field lines at $t = 0$ reflect the preimage of a Hopf fibration from $\mathbb{S}^3 \mapsto \mathbb{S}^2$, so it consists of pairwise linked closed circles lying on nested tori. As can be seen in (Figure 1), these circles get deformed during time evolution correspondingly to (1.9). Looking at (Figure 2), it can clearly be observed that the electric field lines (green) are perpendicular to the magnetic field lines (red) at all displayed times and one can grasp a more general impression about the deformation of the individual field lines during time evolution.

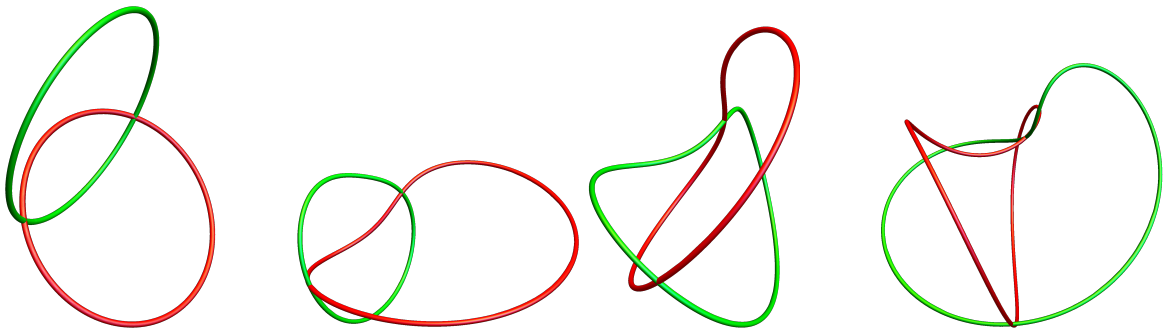

(a) $t = 0$ (b) $t = 0.5$ (c) $t = 1$ (d) $t = 2$

Figure 1: A pair of electric (green) and magnetic (red) field lines for the Hopf-Rañada knot at 4 different times

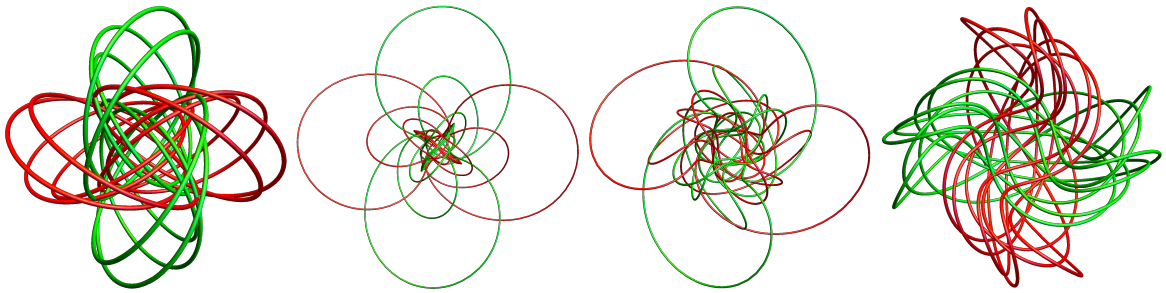

(a) $t = 0$ (b) $t = 0.5$ (c) $t = 1$ (d) $t = 2$

Figure 2: A collection of electric (green) and magnetic (red) field lines for the Hopf-Rañada knot at 4 different times

It turns out, that this particular knot is one of the simplest examples that can be generated with the construction method studied in this thesis. Nonetheless, it is still an interesting object of research to gain further knowledge about null solutions (for example [12]) due to their simplicity and well described structure. Geometrically, null electromagnetic fields are connected to shear-free geodesic congruences in Minkowski space, commonly known as the Robinson theorem and are therefore also interesting objects in the field of differential geometry (for example [13]). Hence it is no surprise, that the results in chapter 4 will be of geometrically and topologically interesting nature.

1.2 Conformal equivalence of dS_4 to $\mathcal{I} \times S^3$ and half of $\mathbb{R}^{1,3}$

De Sitter space is widely known in general relativity as a solution of vacuum Einstein equations with positive cosmological constant and defines a maximally symmetric spacetime of constant positive curvature. It approximates the universe at extremely early times where it rapidly expanded. A brief introduction about the geometry of de Sitter space can be found in [14]. In this thesis, the focus is not on any kind of cosmology but 4-dimensional de Sitter space dS_4 is used as a tool to generate electromagnetic knot solutions in Minkowski space $\mathbb{R}^{1,3}$. Note that this whole construction method described in this chapter, as well as chapter 2 is completely based on [1]. We begin with the main ingredient of this method, that is the conformal equivalence of dS_4 to a real finite cylinder over a 3-sphere $\mathcal{I} \times \mathbb{S}^3$ and half of Minkowski space $\mathbb{R}^{1,3}_{\pm}$.

dS_4 can be realized as a one-sheeted hyperboloid embedded in 5-dimensional Minkowski space $\mathbb{R}^{1,4}$. If we consider the standard Minkowskian metric

$$\mathrm{d}s^2 = -X_0^2 + \sum_{A=1}^{4} \mathrm{d}X_A^2, \tag{1.13}$$

then dS_4 can be parametrized via

$$-X_0^2 + \sum_{A=1}^{4} X_A^2 = l^2, \tag{1.14}$$

where l denotes a non-zero constant with the unit of length. The metric on dS_4 can therefore be described by the induced metric from $\mathbb{R}^{1,4}$. It will be useful to look at equal-time slices of dS_4, that result in 3-spheres of varying radius for each slice. Those slices will be constant X_0-slices depending on a cylinder time coordinate $\tau \in \mathcal{I} = (0, \pi)$. Also, it is useful to introduce four orthogonal coordinates ω_A ($\omega_A \omega_A = 1$) embedding the unit 3-sphere into $\mathbb{R}^4$ with one such embedding could be given for $\chi, \theta \in [0, \pi]$ and $\phi \in [0, 2\pi]$ by

$$\begin{aligned} \omega_1 &= \sin(\chi)\sin(\theta)\sin(\phi)\ , & \omega_2 &= \sin(\chi)\sin(\theta)\cos(\phi)\ , \\ \omega_3 &= \sin(\chi)\cos(\theta)\ , & \omega_4 &= \cos(\chi)\ . \end{aligned} \tag{1.15}$$

If we then choose the parametrization

$$X_0 = -l\cot(\tau) \quad \text{and} \quad X_A = \frac{l}{\sin(\tau)}\omega_A \quad \text{for} \quad A = 1, \ldots, 4\ , \tag{1.16}$$

we obtain the metric

$$\mathrm{d}s^2 = \frac{l^2}{\sin(\tau)^2}(-\mathrm{d}\tau + \mathrm{d}\Omega_3^2). \tag{1.17}$$

This is a sum of the metric of a real cylinder $\mathcal{I}$ and the metric of $\mathbb{S}^3$ scaled by a conformal factor $\frac{l^2}{sin(\tau)^2}$, meaning dS_4 is conformally equivalent to the product $\mathcal{I} \times \mathbb{S}^3$.

This real finite cylinder over a 3-sphere can be further parametrized in such a way, that it is conformally equivalent to the future half $\mathbb{R}^{1,3}_+$ or respectively the past half $\mathbb{R}^{1,3}_-$ of Minkowski space. Introducing Minkowski coordinates $x^\mu = \{t, x, y, z\}$ and $r = \sqrt{x^2 + y^2 + z^2}$, we consider the following parametrization

$$X_0 = \frac{t^2 - r^2 - l^2}{2t}\ ,\ X_1 = l\frac{x}{t}\ ,\ X_2 = l\frac{y}{t}\ ,\ X_3 = l\frac{z}{t}\ ,\ X_4 = \frac{r^2 - t^2 - l^2}{2t}. \tag{1.18}$$

We can observe, that for positive time $t \in \mathbb{R}_+$, it follows that $X_0 + X_4 < 0$, while $t = 0$ is not allowed due to singularity issues. This covers only half of dS_4 and the corresponding metric in Minkowski space then reads

$$\mathrm{d}s^2 = \frac{l^2}{t^2}(-\mathrm{d}t^2 + \mathrm{d}x^2 + \mathrm{d}y^2 + \mathrm{d}z^2). \tag{1.19}$$

We thus obtained the standard metric of 3-dimensional Minkowski space restricted on the future half. Allowing $t \in \mathbb{R}_-$, we can map another half of dS_4 with $X_0 + X_4 > 0$ to the past half of Minkowski space. Via gluing both halfs at $t = \tau = 0$, the whole Minkowski space can be covered so that $t = (-\infty, 0, \infty)$ corresponds to $\tau = (-\pi, 0, \pi)$. This coverage is thus given by two copies of conformally equivalent cylinders over a 3-sphere $2\mathcal{I} \times \mathbb{S}^3$ with $2\mathcal{I} = (-\pi, \pi)$.

A direct relation between cylinder and Minkowski coordinates is obtained by comparing (1.16) and (1.18)

$$\cot\tau = \frac{r^2 - t^2 + l^2}{2lt}, \quad \omega_1 = \gamma\frac{x}{l}, \quad \omega_2 = \gamma\frac{y}{l}, \quad \omega_3 = \gamma\frac{z}{l}, \quad \omega_4 = \gamma\frac{r^2 - t^2 - l^2}{2l^2}, \tag{1.20}$$

where the formulae were simplified by abbreviation of the frequent occurring terms

$$\gamma = \frac{2l^2}{\sqrt{4l^2t^2 + (r^2 - t^2 + l^2)^2}}. \tag{1.21}$$

Whole Minkowski space is only covered by the area bounded by

$$\tau \leq \cos\omega_4, \tag{1.22}$$

what effectively is half of $2\mathcal{I} \times \mathbb{S}^3$. The cylinder time is obtained as a function of Minkowski coordinates by performing the inverse

$$\tau = \mathrm{arccot}(\frac{r^2 - t^2 + l^2}{2lt}). \tag{1.23}$$

From (1.23), we can straightforwardly obtain the relation

$$e^{i\tau} = \frac{(l + \mathrm{i}t)^2 + r^2}{\sqrt{4l^2t^2 + (r^2 - t^2 + l^2)^2}}, \tag{1.24}$$

that will be very helpful later in this thesis. Due to conformal invariance of Yang-Mills theory in 4 dimensions, Maxwell's equations can be solved on $2\mathcal{I} \times \mathbb{S}^3$ rather than on $\mathbb{R}^{1,3}$ and afterwards the obtained solutions can be transformed via a change of coordinates to Minkowski space in order to properly evaluate them. This has the benefits, that finding solutions on de Sitter space turns out to be relatively simple, but the obtained Minkowski solutions are of high complexity, as well as properties concerning finiteness of the action and energy are being conserved. Before starting to study actual electrodynamics on dS_4, the following remark about a generalized approach of solving Yang-Mills equations for arbitrary dimensions that was published in [15] will be made. This is in fact a different field of research but the foundation of the method described in [1] can be regarded as a special case based on this general idea.

Solving Yang-Mills equations on de Sitter spaces dS_{n+1} is a useful tool, because analogously to the special 4-dimensional case described above, a choice of equal-time slices result in a metric describing a real cylinder over a n-sphere $\mathcal{I} \times \mathbb{S}^n$. These unit spheres own interesting structures when considering the maximal compact symmetry subgroup G of the spacetime for solving the Yang-Mills equations. Explicitly, these spheres can be expressed as coset spaces $G \setminus H$ with $H \subset G$ of the following kinds

$$\mathbb{S}^n = \frac{SO(n+1)}{SO(n)}, \quad \mathbb{S}^{2m+1} = \frac{SU(m+1)}{SU(m)}, \quad \mathbb{S}^{4l+3} = \frac{Sp(l+1)}{Sp(l)}. \tag{1.25}$$

It is therefore natural to solve Yang-Mills equations considering the gauge groups $SO(n+1)$, $SU(m+1)$ and $Sp(l+1)$ on dS_{n+1}, dS_{2m+2} and dS_{4l+4} respectively. Such solutions are derived in [15] but due to the non-existing conformal invariance of Yang-Mills theory in arbitrary dimensions, they cannot be simply transformed to Minkowski space. Going back to the space dS_4 where this can be done easily, it is thus natural to work with the group structures of $SO(4)$ and $SU(2)$. Indeed, the focus will be on Maxwell's equations with $U(1) \subset SU(2)$ as gauge group written in a $SO(4)$-covariant formalism reflecting two $su(2)$ algebras on $\mathbb{S}^3$ as can be seen in the next chapter.

2 Generating electromagnetic knot solutions

In this chapter, the correspondence between $2\mathcal{I} \times \mathbb{S}^3$ and $\mathbb{R}^{1,3}$ is used to generate rational electromagnetic knots in Minkowski space. The first step is to derive Maxwell's equations on $2\mathcal{I} \times \mathbb{S}^3$. It turns out that there are two types of solutions that result in a class of infinitely many electromagnetic knot solutions after being transformed to Minkowski space. Some important properties of the solutions will be discussed in detail as well as numerous examples are being visualized at the end of this chapter.

2.1 The formalism

A general ansatz for a gauge potential on $2\mathcal{I} \times \mathbb{S}^3$ can be imposed via

$$\mathcal{A} = X_0(\tau, \omega)\mathrm{d}\tau + \sum_{a=1}^{3} X_a(\tau, \omega)e^a. \tag{2.1}$$

$X_a(\tau, \omega)$ are elements in some associated Lie-algebra $\mathfrak{g}$ for a suitable gauge group G, depending on ω_A and τ and expanded in an orthonormal basis e^a of three left-invariant 1-forms on $\mathbb{S}^3$, satisfying the Maurer-Cartan structure equations

$$\mathrm{d}e^a + \epsilon_{abc}e^b \wedge e^c = 0. \tag{2.2}$$

Given an embedding with coordinates ω_A, these 1-forms can be constructed via

$$e^a = -\eta^a_{BC}\omega_B \mathrm{d}\omega_C \quad \text{with} \quad \eta^a_{BC} = \begin{cases} \epsilon^a_{BC} & \text{for} \quad B, C = 1, 2, 3 \\ +\delta^a_C & \text{for} \quad C = 4 \\ -\delta^a_C & \text{for} \quad B = 4 \\ 0 & \text{for} \quad B = C = 4 \end{cases}. \tag{2.3}$$

The metric of $\mathbb{S}^3$ is then just given by

$$\mathrm{d}\Omega_3^2 = (e^1)^2 + (e^2)^2 + (e^3)^2. \tag{2.4}$$

From now on, the notational convention $e^0 = \mathrm{d}\tau$ will be fixed, resulting in a cleaned up and more structured notation. We also need Minkowski expressions for (2.3), that can be directly computed whilst substituting (1.20). In a compact notation with $x^\mu = (t, x^i) = (t, x, y, z)$ and $i, j, k = \{1, 2, 3\}$, these expressions read

$$e^0(x) = \frac{\gamma^2}{l^3}(\frac{1}{2}(t^2 + r^2 + l^2)\mathrm{d}t - tx^i\mathrm{d}x^i), \tag{2.5}$$

$$e^a(x) = \frac{\gamma^2}{l^3}(tx^a\mathrm{d}t - (\frac{1}{2}(t^2 - r^2 + l^2)\delta^a_k + x^a x^k + l\epsilon^a_{jk}x^j)\mathrm{d}x^k). \tag{2.6}$$

In order to work in a gauge theory with $G = U(1)$ and $\mathfrak{g} = \mathbb{R}$ on $2\mathcal{I} \times \mathbb{S}^3$, a formalism that captures the dependence of the functions $X_a(\tau, \omega)$ on the spherical coordinates

while being $SO(4)$-covariant is constructed in terms of the following representations of two $su(2)$-algebras

$$R_a = -\eta^a_{BC}\omega_B \frac{\partial}{\partial \omega_c} \quad \text{with} \quad [R_a, R_b] = 2\epsilon_{abc}R_c \ , \tag{2.7}$$

$$L_a = -\tilde{\eta}^a_{BC}\omega_B \frac{\partial}{\partial \omega_c} \quad \text{with} \quad [L_a, L_b] = 2\epsilon_{abc}L_c \ . \tag{2.8}$$

Here, R_a define three left-invariant vector fields generating right translations and L_a define three right-invariant vector fields generating left translations that mutually commute

$$[R_a, L_b] = 0. \tag{2.9}$$

It can also be observed that

$$L_a e^a = 0 \quad \text{and} \quad e^a R_b = \delta^a_b, \tag{2.10}$$

hence (2.7) defines a basis dual to e^a. The space of functions on $\mathbb{S}^3$ is given by irreducible representations of the sum

$$su(2)_L \oplus su(2)_R \tag{2.11}$$

generating left and right translations on $\mathbb{S}^3$ with the restriction that they have to be labeled by a common spin $j = 0, \frac{1}{2}, 1, \frac{3}{2}, \ldots$. Per definition (2.3) and (2.7), the exterior derivative of an arbitrary function $\Phi(\omega_A)$ on $\mathbb{S}^3$ can be expressed as

$$\mathrm{d}\Phi = e^a R_a \Phi(\omega_A). \tag{2.12}$$

A basis of functions on $\mathbb{S}^3$ is given by hyperspherical harmonics $Y_{j;m,n}$ in an analogue fashion to $\mathbb{S}^2$ with its basis of spherical harmonics. They depend on two labels $m, n = -j, -j+1, \ldots, +j$ arising from (2.11) and a common labeled spin j. This formalism reminds of the language commonly used in quantum mechanics and hence it is natural to formally introduce hermitian angular-momentum operators

$$I_a := \frac{\mathrm{i}}{2} L_a \quad \text{and} \quad J_a := \frac{\mathrm{i}}{2} R_a, \tag{2.13}$$

so the basis of hyperspherical harmonics is specified by the following eigenvalue relations

$$I^2 Y_{j;m,n} = J^2 Y_{j;m,n} = j(j+1) Y_{j;m,n} \ , \tag{2.14}$$

$$I_3 Y_{j;m,n} = m Y_{j;m,n} \quad \text{and} \quad J_3 Y_{j;m,n} = n Y_{j;m,n}. \tag{2.15}$$

It will be convenient to employ the notation of ascending and descending operators acting on m and n respectively

$$I_\pm = \frac{1}{\sqrt{2}}(I_1 \pm \mathrm{i} I_2) \ \text{ and } \ J_\pm = \frac{1}{\sqrt{2}}(J_1 \pm \mathrm{i} J_2) \tag{2.16}$$

so that they act on the basis of hyperspherical harmonics as

$$J_{\pm}Y_{j;m,n} = \sqrt{j(j+1) - n(n\pm 1)}Y_{j;m,n\pm 1}, \tag{2.17}$$

$$I_{\pm}Y_{j;m,n} = \sqrt{j(j+1) - m(m\pm 1)}Y_{j;m\pm 1,n}. \tag{2.18}$$

We can define angles $\{\alpha, \bar{\alpha}, \beta, \bar{\beta}\}$ on $\mathbb{S}^3$ satisfying $\bar{\alpha}\alpha + \bar{\beta}\beta = 1$ via

$$\begin{aligned} \alpha &= \omega_1 + \mathrm{i}\omega_2 \ , & \beta &= \omega_3 + \mathrm{i}\omega_4 \ , \\ \bar{\alpha} &= \omega_1 - \mathrm{i}\omega_2 \ , & \bar{\beta} &= \omega_3 - \mathrm{i}\omega_4 \ . \end{aligned} \tag{2.19}$$

If we then use (2.13) and (2.16) together with (2.19), we obtain

$$\begin{aligned} I_+ &= \frac{1}{\sqrt{2}}(\bar{\beta}\partial_{\bar{\alpha}} - \alpha\partial_{\beta}) \ , & J_+ &= \frac{1}{\sqrt{2}}(\beta\partial_{\bar{\alpha}} - \alpha\partial_{\bar{\beta}}) \ , \\ I_3 &= \frac{1}{2}(\alpha\partial_{\alpha} + \bar{\beta}\partial_{\bar{\beta}} - \bar{\alpha}\partial_{\bar{\alpha}} - \beta\partial_{\beta}) \ , & J_3 &= \frac{1}{2}(\alpha\partial_{\alpha} + \beta\partial_{\beta} - \bar{\alpha}\partial_{\bar{\alpha}} - \bar{\beta}\partial_{\bar{\beta}}) \ , \\ I_- &= \frac{1}{\sqrt{2}}(\bar{\alpha}\partial_{\bar{\beta}} - \beta\partial_{\alpha}) \ , & J_- &= \frac{1}{\sqrt{2}}(\bar{\alpha}\partial_{\beta} - \bar{\beta}\partial_{\alpha}) \ . \end{aligned} \tag{2.20}$$

An explicit expression for the normalized hyperspherical harmonics is given by

$$Y_{j;m,n} = \sqrt{\frac{2j+1}{2\pi^2}}\sqrt{\frac{2^{j-m}(j+m)!}{(2j)!(j-m)!}\frac{2^{j-n}(j+n)!}{(2j)!(j-n)!}}(I_-)^{j-m}(J_-)^{j-n}\alpha^{2j}, \tag{2.21}$$

where the terms under the square root are normalization constants and the following descending operators acting on α^{2j} result in homogeneous polynomials of degree $2j$ in $\alpha, \bar{\alpha}, \beta, \bar{\beta}$. In order to compute (2.21), it is effectively needed to first compute

$$(J_-)^{j-n}\alpha^{2j} = (\frac{-\bar{\beta}}{\sqrt{2}})^{j-n}\partial_{\alpha}^{j-n}\alpha^{2j} =: g(\alpha, \bar{\beta}) \tag{2.22}$$

followed by corresponding derivatives depending on the order $j - m$, for example

$$I_-g(\alpha, \bar{\beta}) = \frac{1}{\sqrt{2}}(\bar{\alpha}\partial_{\bar{\beta}} - \beta\partial_{\alpha})g(\alpha, \bar{\beta}), \tag{2.23}$$

$$I_-(I_-g(\alpha, \bar{\beta})) = \frac{1}{2}(\bar{\alpha}^2\partial_{\bar{\beta}}^2 + \beta^2\partial_{\alpha}^2 - 2\bar{\alpha}\beta\partial_{\bar{\beta}}\partial_{\alpha})g(\alpha, \bar{\beta}), \tag{2.24}$$

$$I_-((I_-)^2g(\alpha, \bar{\beta})) = \frac{1}{2\sqrt{2}}(\bar{\alpha}^3\partial_{\bar{\beta}}^3 - \beta^3\partial_{\alpha}^3 + 3\bar{\alpha}\beta^2\partial_{\bar{\beta}}\partial_{\alpha}^2 - 3\bar{\alpha}^2\beta\partial_{\bar{\beta}}^2\partial_{\alpha})g(\alpha, \bar{\beta}). \tag{2.25}$$

Those orders of $(I_-)^{j-m}$ are needed in order to compute solutions for $j = \frac{1}{2}, 1, \frac{3}{2}$. Note that depending on the quantum numbers, one has to deal with factorials of negative numbers. The hyperspherical harmonics will later serve as an orthonormal basis for the Maxwell solutions due to their orthonormality property given by

$$\int_{\mathbb{S}^3} Y^*_{j;m,n}Y_{j';m',n'}\mathrm{d}^3\Omega_3 = \delta_{jj'}\delta_{mm'}\delta_{nn'} \quad \text{with} \quad Y^*_{j;m,n} = (-1)^{m+n}Y_{j;-m,-n}. \tag{2.26}$$

2.2 Maxwell's equations on $2\mathcal{I} \times \mathbb{S}^3$

The gauge for (2.1) will be fixed with the temporal gauge and Coulomb gauge conditions on $2\mathcal{I} \times \mathbb{S}^3$ given by

$$X_0(\tau, \omega) = 0 \quad \text{and} \quad J_a X_a(\tau, \omega) = 0, \tag{2.27}$$

resulting in $\mathcal{A}_\tau$=0. Using (2.12) and a rewritten form of (2.2)

$$\mathrm{d}e^a = -\epsilon_{abc} e^b \wedge e^c, \tag{2.28}$$

the curvature $\mathcal{F}$ can be computed as follows

$$\begin{aligned} \mathcal{F} = \mathrm{d}\mathcal{A} &= \mathrm{d}X_a e^a + X_a \mathrm{d}e^a \\ &= \dot{X}_a e^0 \wedge e^a + R_a X_b e^a \wedge e^b - \epsilon_{abc} X_a e^b \wedge e^c \\ &= -\dot{X}_a e^a \wedge e^0 + \frac{1}{2}(R_{[a} X_{b]} - 2\epsilon_{abc} X_c) e^a \wedge e^b \ . \end{aligned} \tag{2.29}$$

We can observe, that (2.29) resembles the familiar structure of the field strength tensor in Minkowski space and indeed it is the analogue quantity of this tensor in $2\mathcal{I} \times \mathbb{S}^3$. Denoting $\mathcal{F}_{a0} = \mathcal{E}_a$ and $\frac{1}{2}\epsilon_{abc}\mathcal{F}_{bc} = \mathcal{B}_a$, we can directly read the analogue quantities of electric and magnetic fields in de Sitter space

$$\mathcal{E}_a = -\dot{X}_a \ \text{ and } \ \mathcal{B}_a = \epsilon_{abc} R_b X_c - 2X_a. \tag{2.30}$$

The vacuum Maxwell's equations are given by

$$\mathrm{d}\mathcal{F} = \mathrm{d} \star \mathcal{F} = 0, \tag{2.31}$$

so we first need to compute the Hodge dual

$$\begin{aligned} \star\mathcal{F} &= \frac{1}{2}\dot{X}_a \epsilon_{abc} e^b \wedge e^c - \epsilon_{abc} R_a X_b e^0 \wedge e^c + \epsilon_{abc}\epsilon_{bcd} X_a e^0 \wedge e^d \\ &= \frac{1}{2}\dot{X}_a \epsilon_{abc} e^b \wedge e^c - \epsilon_{abc} R_a X_b e^0 \wedge e^c + 2X_a e^0 \wedge e^a \end{aligned} \tag{2.32}$$

followed by the exterior derivative

$$\begin{aligned} \mathrm{d} \star \mathcal{F} =& \frac{1}{2}(\ddot{X}_a \epsilon_{abc} e^0 \wedge e^b \wedge e^c + R_d \dot{X}_a \epsilon_{abc} e^d \wedge e^b \wedge e^c) + \epsilon_{abc} R_d R_a X_b e^0 \wedge e^d \wedge e^c \\ &- \epsilon_{abc}\epsilon_{0de} R_a X_b e^0 \wedge e^d \wedge e^e + 2(X_a \epsilon_{abc} e^0 \wedge e^b \wedge e^c + R_a X_b e^0 \wedge e^b \wedge e^a). \end{aligned} \tag{2.33}$$

The Gauss law on $2\mathcal{I} \times \mathbb{S}^3$ can be found as

$$\frac{1}{2} R_a \dot{X}_a = 0 \tag{2.34}$$

and substituting (2.34) into (2.33) leads after some index rearranging to a compact expression for (2.31) reading

$$\begin{aligned} -\frac{1}{4}\ddot{X}_a &= -\frac{1}{4}R^2 X_a + X_a - \frac{1}{2}\epsilon_{abc} R_b X_c + \frac{1}{4} R_a R_b X_b \\ &= (J^2 + 1) X_a + \mathrm{i}\epsilon_{abc} J_b X_c - J_a J_b X_b. \end{aligned} \tag{2.35}$$

With the fixed gauge (2.27), the last term vanishes and this simplifies to the final form of Maxwell's equations on $2\mathcal{I} \times \mathbb{S}^3$

$$-\frac{1}{4}\ddot{X}_a = (J^2+1)X_a + \mathrm{i}\epsilon_{abc}J_bX_c, \tag{2.36}$$

what corresponds to the three equations

$$-\frac{1}{4}\ddot{X}_1 = (J^2+1)X_1 + \mathrm{i}(J_2X_3 - J_3X_2), \tag{2.37}$$

$$-\frac{1}{4}\ddot{X}_2 = (J^2+1)X_2 + \mathrm{i}(J_3X_1 - J_1X_3), \tag{2.38}$$

$$-\frac{1}{4}\ddot{X}_3 = (J^2+1)X_3 + \mathrm{i}(J_1X_2 - J_2X_1). \tag{2.39}$$

At this point, we are now interested in finding explicit solutions for (2.36), that will be the field configurations creating all kinds of interesting knotted electromagnetic fields. Following this task, we first define

$$X_\pm = \frac{1}{\sqrt{2}}(X_1 \pm \mathrm{i}X_2)\ , \tag{2.40}$$

staying in the same language as (2.16) and rewrite the equations of motion in terms of $X_\pm$ and X_3. This yields the following system of equations (Appendix 6.1.1)

$$\begin{aligned} -\frac{1}{4}\ddot{X}_+ &= (J^2 - J_3 + 1)X_+ + J_+X_3, \\ -\frac{1}{4}\ddot{X}_- &= (J^2 + J_3 + 1)X_- - J_-X_3, \\ -\frac{1}{4}\ddot{X}_3 &= (J^2+1)X_3 - J_+X_- + J_-X_+, \end{aligned} \tag{2.41}$$

together with a rewritten form of the initial gauge condition

$$0 = J_3X_3 + J_+X_- + J_-X_+. \tag{2.42}$$

The first step of solving these equations can be done with a seperation ansatz

$$X_a(\tau,\omega) = \sum_{j,m,n} X_a^{j;m,n}(\tau)Y_{j;m,n}(\alpha,\bar{\alpha},\beta,\bar{\beta}), \tag{2.43}$$

where the field configurations are expanded as τ-dependent parts in the orthonormal basis of hyperspherical harmonics. From (2.41) and (2.42), it then can be observed that

$$X_3 \propto Y_{j;m,n} \Rightarrow X_\pm \propto J_\pm X_3. \tag{2.44}$$

Thus, Maxwell's equations are coupled equations for $\{X_+^{j,m,n+1}, X_-^{j;m,n-1}, X_3^{j;m,n}\}$. This means also that j and m can be fixed, what is not surprising for a formalism build around solely on the action of R_a and J_a correspondingly. In order to decouple (2.41),

we additionally impose an exponential ansatz for the cylinder parts of $X_a(\tau,\omega)$ given by

$$X_a(\tau) = e^{\mathrm{i}\Omega_a^{j;n}\tau} c_a^{j;n}. \tag{2.45}$$

Using (2.41)-(2.45) together with (2.14),(2.15) and (2.17), we are left with a linear system of ordinary differential equations for the frequencies $\Omega_a^{j;n}$ and amplitudes $c_a^{j;n}$ that can be solved with the standard method.

We obtain two families of solutions distinguished by their value of the integral frequency that only depends on j

$$\Omega_j = \pm 2(j+1) \quad \text{or} \quad \Omega_j = \pm 2j, \tag{2.46}$$

which will be called basis solutions of type I and type II. They each individually have different amplitudes $c_a^{j;n}$ and obey different ranges for m and n, but as can be seen in a moment, they are both connected by a remarkably simple transformation. Below one can see the explicit solutions for (2.41) of both types.

Type I: $j \geq 0$, $m = -j, \ldots, +j$, $n = -j-1, \ldots, j+1$, $\Omega^j = \pm 2(j+1)$

$$\begin{aligned} X_+ &= \sqrt{\frac{1}{2}(j-n)(j-n+1)}\, e^{\pm 2(j+1)\mathrm{i}\tau} Y_{j;m,n+1} \ , \\ X_- &= -\sqrt{\frac{1}{2}(j+n)(j+n+1)}\, e^{\pm 2(j+1)\mathrm{i}\tau} Y_{j;m,n-1} \ , \\ X_3 &= \sqrt{(j+1)^2 - n^2}\, e^{\pm 2(j+1)\mathrm{i}\tau} Y_{j;m,n} \ . \end{aligned} \tag{2.47}$$

Type II: $j \geq 1$, $m = -j, \ldots, +j$, $n = -j+1, \ldots, j-1$, $\Omega^j = \pm 2j$

$$\begin{aligned} X_+ &= -\sqrt{\frac{1}{2}(j+n)(j+n+1)}\, e^{\pm 2j\mathrm{i}\tau} Y_{j;m,n+1} \ , \\ X_- &= \sqrt{\frac{1}{2}(j-n)(j-n+1)}\, e^{\pm 2j\mathrm{i}\tau} Y_{j;m,n-1} \ , \\ X_3 &= \sqrt{j^2 - n^2}\, e^{\pm 2j\mathrm{i}\tau} Y_{j;m,n} \ . \end{aligned} \tag{2.48}$$

Counting out all possible solutions for fixed j of type I, there are $(2j+1)$ possible values for m and $(2j+3)$ values for n. Because the basis solutions are complex and real and imaginary parts solve Maxwell's equations independently, there are $2(2j+1)(2j+3)$ real linearly independent type I solutions in total. With the same way of counting, we see that there are $2(2j+1)(2j-1)$ real linearly independent type II solutions. Note that due to linearity of Maxwell's equations, sums of individual solutions again solve

them, so in general we are also interested in all the superpositions of solutions for fixed j. A formalism that resembles such general superpositions as well as the nature that real and imaginary parts solve Maxwell's equations separately is given by

$$X_a = c_a e^{+\mathrm{i}\Omega_j \tau} + c_a^* e^{-\mathrm{i}\Omega_j \tau} \quad \text{with} \quad c_a = \sum_{m,n} c_{mn} Z_a^{mn}. \tag{2.49}$$

Here, Z_a^{mn} denote the hyperspherical harmonics together with the amplitudes for every solution X_a in the basis of $a = \{+, -, 3\}$ or $\{1, 2, 3\}$, whereas c_{mn} are some complex coefficients chosen for every combination of m and n corresponding to a solution with fixed j. The change of basis for X_a is simply realized via

$$X_1 = \frac{1}{\sqrt{2}}(X_+ + X_-) \quad \text{and} \quad X_2 = \frac{1}{\sqrt{2}\mathrm{i}}(X_+ - X_-) \tag{2.50}$$

and will be the preferred basis from now on. The complex conjugated $\bar{Z}_a^{mn}$ are obtained through swapping $\alpha \leftrightarrow \bar{\alpha}$, $\beta \leftrightarrow \bar{\beta}$ and keeping into account all sign changes that come from every factor of i, resulting in (2.26). The corresponding gauge potential to (2.49) is then given by

$$\mathcal{A} = (c_{mn} Z_a^{mn} e^{\mathrm{i}\Omega_j \tau} + c_{mn}^* \bar{Z}_a^{mn} e^{-\mathrm{i}\Omega_j \tau}) e^a. \tag{2.51}$$

There are two major ways transforming the de Sitter solutions to electromagnetic fields in Minkowski space, as one can see in the chart below:

$$\begin{array}{ccc} \mathcal{A}_a e^a & \xrightarrow{X_a(\tau(x),\omega(x)) e_\mu^a(x) \mathrm{d}x^\mu} & A_\mu \mathrm{d}x^\mu \\ \Big\downarrow \mathrm{d}\mathcal{A} & & \Big\downarrow \mathrm{d}A \\ \frac{1}{2}\mathcal{F}_{ab} e^a \wedge e^b & \xrightarrow{\frac{1}{2}\mathcal{F}_{ab}(\tau(x),\omega(x)) e_{\mu\nu}^{ab}(x) \mathrm{d}x^\mu \wedge \mathrm{d}x^\nu} & \frac{1}{2} F_{\mu\nu} \mathrm{d}x^\mu \wedge \mathrm{d}x^\nu \end{array} . \tag{2.52}$$

The first way would be to go right and begin by transforming $\mathcal{A}$ to Minkowski space via the coordinate transformation

$$\mathcal{A} = X_a(\tau, \omega) e^a = X_a(\tau(x), \omega(x)) e_\mu^a(x) \mathrm{d}x^\mu = A_\mu \mathrm{d}x^\mu, \tag{2.53}$$

where the Minkowski expressions $\tau(x)$ for the τ-dependent parts are given by (1.24) and the Minkowski expressions $\omega(x)$ for the spherical parts are given by substituting (2.19) together with (1.20) into (2.21). The resulting terms then have to be sorted to determine the components A_μ. Afterwards we can compute the field strength tensor

$$F = \mathrm{d}A = \frac{1}{2} F_{\mu\nu} \mathrm{d}x^\mu \wedge \mathrm{d}x^\nu \tag{2.54}$$

and directly read the field expressions F_{i0} and F_{ij} or we can compute its components from the gauge potential via

$$F_{\mu\nu} = \partial_\mu A_\nu - \partial_\nu A_\mu. \tag{2.55}$$

We can also go down at first in the chart and then perform the coordinate transformation

$$\frac{1}{2}\mathcal{F}_{ab}e^a \wedge e^b = \frac{1}{2}\mathcal{F}_{ab}(\tau(x), \omega(x))e^{ab}_{\mu\nu}(x)\mathrm{d}x^\mu \wedge \mathrm{d}x^\nu. \tag{2.56}$$

After doing that, again the resulting terms have to be sorted in order to read the components $F_{\mu\nu}$.

The solutions will always result in rational functions in Minkowski space, even for odd powers of $e^{\mathrm{i}\Omega_j\tau}$. This justifies why these solutions are called rational electromagnetic knots. Even though the computation of the change of coordinates for a simple solution can be done straightforwardly per hand, it is recommended doing this work with a programmed routine, as most of the solutions will result in long and complicated expressions, that are hard being computed manually in a reasonable time frame. In (Appendix 6.2.1), a routine written in Mathematica is presented, that was used for all such computations occurring in this thesis.

Before getting more involved with the further discussion of these electromagnetic solutions, some general structural properties that can be directly derived from (2.47) and (2.48) are being listed in the next section.

2.3 Properties of the solutions

We can observe, that spin j type I solutions are linked to spin $j+1$ type II solutions via a parity transformation $m \leftrightarrow n$ exchanging left- and right algebras on $\mathbb{S}^3$. Also producing dual solutions of type I (type II)

$$\mathcal{B}_D = \mathcal{E} \quad \text{and} \quad \mathcal{E}_D = -\mathcal{B} \tag{2.57}$$

just works by shifting the frequency $|\Omega_j|\tau$ by $\frac{\pi}{2}$ $(-\frac{\pi}{2})$, what effectively results in

$$X^D_a = \pm \mathrm{i}c_a e^{\mathrm{i}\Omega_j\tau} \mp \mathrm{i}c^*_a e^{-\mathrm{i}\Omega_j\tau}. \tag{2.58}$$

Here the upper sign belongs to the type I solutions and the lower sign to the type II solutions. This notation will be used for all computations involving type I and type II solutions. The dual solutions (2.57) and (2.58) will be useful for computing the magnetic helicity in chapter 3, revealing a linear dependency between energy and electromagnetic helicity. Naturally, null solutions are contained in (2.47) and (2.48), so with this method, a large number of knots with fascinating geometric properties as described in the introduction were found.

As was mentioned at the beginning of this thesis, this construction guarantees finite action and energy. One simple way to enlighten that the latter is indeed true in Minkowski space, is by observing that the obtained electromagnetic fields in Minkowski space have a power law decay. For this we need to check the asymptotic behaviour of $\mathcal{F}$.

Considering $r \to \infty$ for a fixed time, this corresponds to approaching the point $\omega_4 = 1$

on $\mathbb{S}^3$, therefore the hyperspherical harmonics and as a consequence the solutions X_a tend to some constant value. As in this limit

$$\{e^0, e^a\} \propto \frac{1}{r^2} \Rightarrow e^0 \wedge e^a \propto \frac{1}{r^4} \quad \text{and} \quad e^b \wedge e^c \propto \frac{1}{r^4}, \tag{2.59}$$

we obtain a power law decay for the electric and magnetic fields

$$E_i \propto \frac{1}{r^4} \quad \text{and} \quad B_i \propto \frac{1}{r^4}. \tag{2.60}$$

Analogously, considering fields on the whole light cone ($r = t \to \infty$ for the future half or $r = -t \to \infty$ for the past half) leads to a decay law given by

$$E_i \propto \frac{1}{r} \quad \text{and} \quad B_i \propto \frac{1}{r}. \tag{2.61}$$

The basis of hyperspherical harmonics therefore yields sufficiently fast temporally and spatially decaying fields.

Another benefit is, that only finite time dynamics are needed on $2\mathcal{I} \times \mathbb{S}^3$ for generating knots with infinite time dynamics on Minkowski space. This opens up the possibility to first transform a solution that is known in Minkowski space for $t = 0$ to de Sitter space at $\tau = 0$ and then evaluate the time dynamics there. Afterwards, the solution can be transformed back to Minkowski space, yielding infinite time dynamics there.

2.4 $SO(4)$-invariant solutions

The simplest kinds of solutions are given for $j = 0$ type I and $j = 1$ type II correspondingly. In those cases, the hyperspherical harmonics are real $Z_a^{mn} = \bar{Z}_a^{mn}$ and thus the configurations for type I solutions result in

$$X_a^{j=0} = c_{mn} e^{2\mathrm{i}\tau} + c_{mn}^* e^{-2\mathrm{i}\tau}, \tag{2.62}$$

yielding general superpositions of configurations from $\cos(2\tau)$ and $\sin(2\tau)$. Those are completely independent of the spherical coordinates, hence they are $SO(4)$-invariant. These solutions could likewise be obtained in a limited framework by initially imposing $X_a(\tau, \omega) = X_a(\tau)$ before deriving the equations of motion for X_a. In this case, the curvature computes to

$$\mathcal{F} = \dot{X}_a(\tau) e^0 \wedge e^a - \epsilon_{abc} X_a(\tau) e^b \wedge e^c$$

and the analogue quantities of electric and magnetic fields in de Sitter space follow as

$$\mathcal{E}_a = -\dot{X}_a(\tau) \quad \text{and} \quad \mathcal{B}_a = -2X_a(\tau). \tag{2.63}$$

As can be seen in [16], the general Yang-Mills equations on $2\mathcal{I} \times S^3$ read

$$-\ddot{X}_a = -4X_a + 3\epsilon_{abc}[X_b, X_c] - [X_b, [X_a, X_b]] \quad \text{and} \quad [\dot{X}_a, X_a] = 0, \tag{2.64}$$

what reduces in the abelian case with $[X_b, X_c] = [X_b, [X_a, X_b]] = 0$ and $\mathfrak{g} = \mathbb{R}$ to the differential equations

$$-\ddot{X}_a(\tau) = -4X_a(\tau). \tag{2.65}$$

A general solution of (2.65) is then given by oscillations depending on 6 integration constants c_a and τ_a

$$X_a(\tau) = c_a \cos(2(\tau - \tau_a)). \tag{2.66}$$

These oscillating solutions can be rewritten as

$$\begin{aligned} X_a(\tau) &= c_a \frac{1}{2}(e^{2\mathrm{i}(\tau-\tau_a)} + e^{-2\mathrm{i}(\tau-\tau_a)}) \\ &= c_a \frac{1}{2}(e^{2\mathrm{i}\tau}\tau_{a-} + e^{-2\mathrm{i}\tau}\tau_{a+}) \end{aligned} \tag{2.67}$$

where $\tau_{a-} = e^{-2\mathrm{i}\tau_a}$ and $\tau_{a+} = e^{2\mathrm{i}\tau_a}$. Obviously they are all contained in (2.62). As a simple example setting $l = 1$, we can generate the Hopf-Rañada knot mentioned in the introduction before with the configurations

$$X_1(\tau) = -\frac{1}{8}\sin(2\tau), \qquad X_2(\tau) = -\frac{1}{8}\cos(2\tau), \qquad X_3(\tau) = 0. \tag{2.68}$$

An evident advantage of generating the Hopf-Rañada knot with this method, is that the gauge potential in Minkowski space

$$\begin{aligned} A_0 &= \frac{1}{4} it \left(\frac{-x + iy}{((l + it)^2 + r^2)^2} + \frac{x + iy}{((l - it)^2 + r^2)^2} \right), \\ A_1 &= \frac{1}{8} \left(\frac{2(-t + x(y + ix) + z + i)}{((1 + it)^2 + x^2 + y^2 + z^2)^2} - \frac{i}{(1 + it)^2 + r^2} + \frac{2(-t + x(y - ix) + z - i)}{(-(t + i)^2 + r^2)^2} + \frac{i}{-(t + i)^2 + r^2} \right), \\ A_2 &= \frac{1}{8} \left(\frac{2(i(t - z) + y(y + ix) + 1)}{((1 + it)^2 + r^2)^2} - \frac{1}{-(t + i)^2 + r^2} - \frac{2i(t + y(x + iy) - z + i)}{(-t(t + 2i) + r^2 + 1)^2} - \frac{1}{(1 + it)^2 + r^2} \right), \\ A_3 &= \frac{1}{4} \left(\frac{(z - i)(y - ix)}{(-t(t + 2i) + r^2 + 1)^2} + \frac{(z + i)(y + ix)}{(-t(t - 2i) + r^2 + 1)^2} \right) \end{aligned}$$

is readily computed. This holds for every solution that can be generated with this method and gives direct access to information, previous methods are lacking.

The more interesting cases are given with a non-trivial dependence on the $\mathbb{S}^3$ coordinates and will start at $j = \frac{1}{2}$ type I and $j = \frac{3}{2}$ type II correspondingly.

2.5 Examples and visualizations

In this section, there will be given some non-trivial examples of type I solutions with corresponding visualizations of their electric and magnetic field lines in Minkowski space, to gain a better understanding of what kinds of solutions can actually be found using this formalism. Up to this point, there was only shown a single $SO(4)$-symmetric solution. Note that this is only a qualitative overview about some of the solutions. For each solution there are infinitely many field lines and here are only shown some specific configurations of those lines for a fixed time. Nonetheless, these images reveal some particular information about the structure of the knots as well as how drastically those structures change when evolving through time.

At first the solutions are computed in the basis of hyperspherical harmonics, then transformed to Minkowski space and after explicit expressions for the electric and magnetic fields are obtained, we can solve

$$\frac{\mathrm{d}\vec{r}(s)}{\mathrm{d}s} = \alpha\vec{E}(\vec{r}(s))\Big|_{t=t_0} \quad \text{and} \quad \frac{\mathrm{d}\vec{r}(s)}{\mathrm{d}s} = \alpha\vec{B}(\vec{r}(s))\Big|_{t=t_0}. \tag{2.69}$$

Here $\vec{r}(s)$ is a vector curve corresponding to the field lines of $\vec{E}$ and $\vec{B}$ evaluated at a fixed time t_0 and α denotes a normalization constant. To obtain a useful collection of field lines, we need to fix a suitable set of initial conditions $\{x_0, y_0, z_0\}$ and find a suitable range for varying the curve parameter s. The Mathematica code for this process is shown in (Appendix 6.2.2) together with an online source, where the implementation of (2.69) written by Jens Nöckel can be found. All solutions given in this section were computed for a de Sitter scale of $l = 1$.

The first example will be another one of the six $j = 0$ solutions given by

$$\{0, 0, 0\} = \frac{1}{2\pi}\{0, 0, \cos 2\tau\}. \tag{2.70}$$

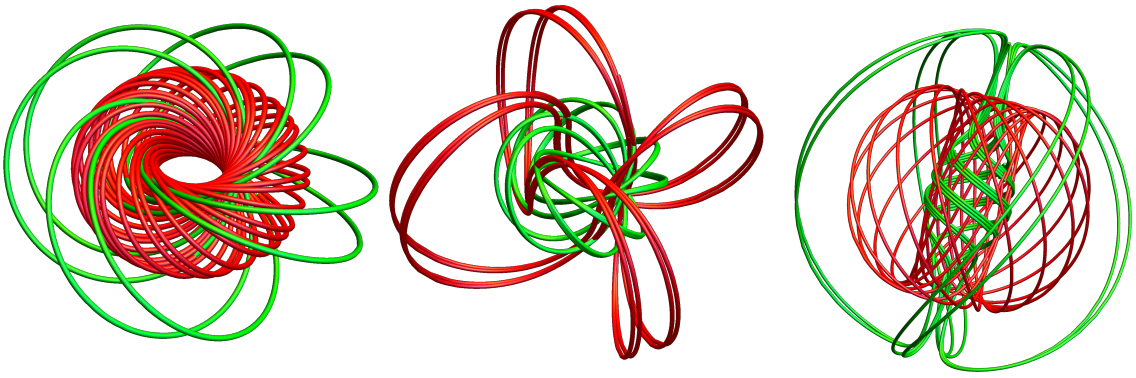

(a) $t = 0.01$ (b) $t = 1$ (c) $t = 2.5$

Figure 3: Some electric and magnetic field line configurations for a $\{0, 0, 0\}$ solution at 3 different times

From (Figure 3), we can observe, that the magnetic field lines at $t \approx 0$ form closed circles on a torus as we have seen from the Hopf-Rañada knot and that the electric field lines wind up on a smaller torus sharing the same boundary of the torus hole. Considering the evolution in time, the structure changes quite a bit and a detail worth mentioning there, is that inner and outer position of the electric and magnetic fields interchange here. This is truly an example on how different such a field evolves when compared to the time evolution of a null field.

The following solution will be the first one with a non-trivial dependence on the $\mathbb{S}^3$ coordinates and additionally satisfies the null condition.

$$\{\frac{1}{2},\frac{1}{2},\frac{3}{2}\} : \frac{1}{2\mathrm{i}}(\left\{-\frac{\sqrt{\frac{3}{2}}\alpha}{\pi},-\frac{\mathrm{i}\sqrt{\frac{3}{2}}\alpha}{\pi},0\right\}e^{3\mathrm{i}\tau}-\left\{-\frac{\sqrt{\frac{3}{2}}\bar{\alpha}}{\pi},\frac{\mathrm{i}\sqrt{\frac{3}{2}}\bar{\alpha}}{\pi},0\right\}e^{-3\mathrm{i}\tau}). \tag{2.71}$$

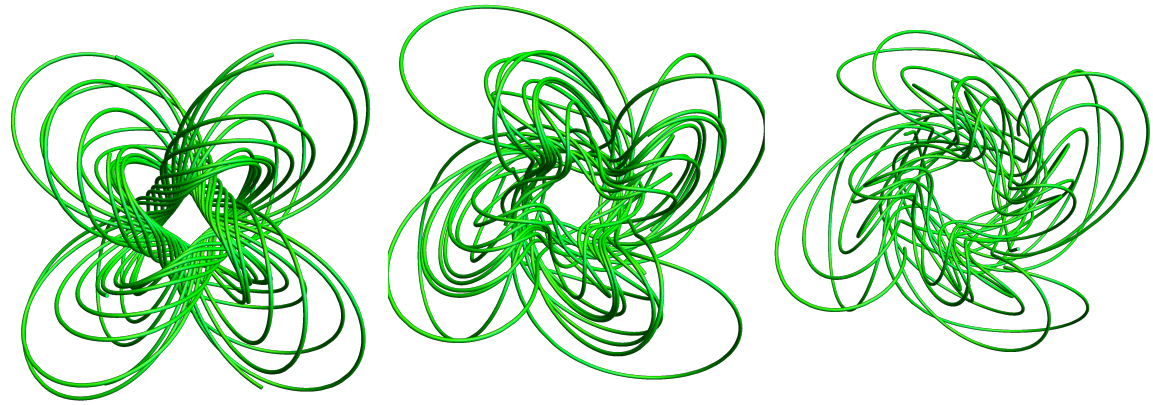

(a) $t = 0$ (b) $t = 0.75$ (c) $t = 1.25$

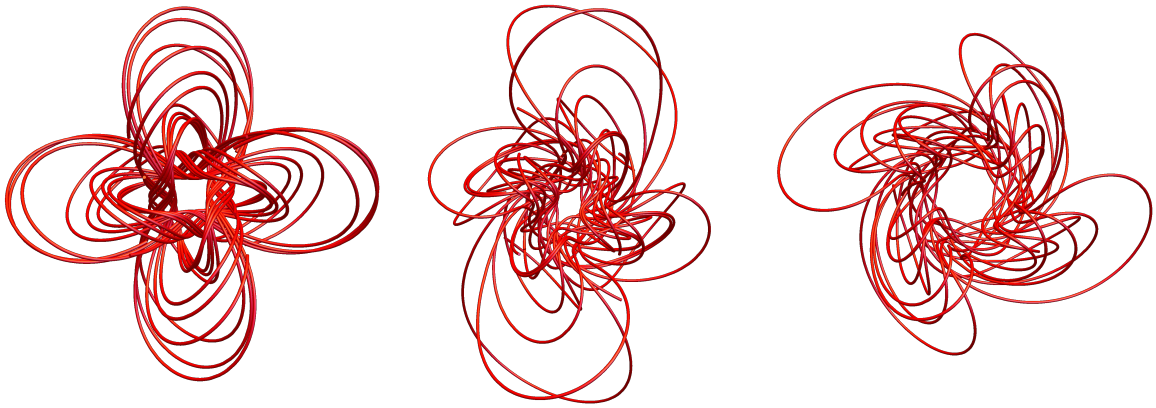

(d) $t = 0$ (e) $t = 0.75$ (f) $t = 1.25$

Figure 4: Electric ((a)-(c)) and magnetic ((d)-(f)) field line configurations for a $\{\frac{1}{2},\frac{1}{2},\frac{3}{2}\}$ solution at 3 different times

From the corresponding Riemann-Silberstein vector

$$\vec{F} = \frac{12\sqrt{6}l^3}{\pi\left((l-\mathrm{i}t)^2+r^2\right)^4}\begin{pmatrix} -(x+\mathrm{i}y)(l-\mathrm{i}(t+x+\mathrm{i}y-z))(l-\mathrm{i}t+\mathrm{i}x-y+\mathrm{i}z) \\ (y-\mathrm{i}x)(l-\mathrm{i}(t-\mathrm{i}x+y-z))(l-\mathrm{i}t+x+\mathrm{i}(y+z)) \\ 2(x+\mathrm{i}y)^2(\mathrm{i}l+t-z) \end{pmatrix},$$

it can clearly be seen that (2.71) is indeed a null field. This time the electric and magnetic field lines were split up, otherwise the visualizations would look too chaotic. Also for those solutions a view from the top was chosen to better grasp the knotted structure and symmetry. From (Figure 4), we can observe that the evolution in time for both electric and magnetic field lines happens via smooth deformations as was shown in the introduction for the Hopf-Rañada knot. However, the perpendicularity of the electric and magnetic field lines is not obvious from those pictures, so maybe one need to find a suitable set of initial conditions in order to better illustrate this.

The next example shows a different characteristic that can be found in the set of $j = \frac{1}{2}$ solutions. Let us consider

$$\{\frac{1}{2}, \frac{1}{2}, -\frac{1}{2}\} : \left\{\frac{\alpha}{\sqrt{2}\pi}, -\frac{i\alpha}{\sqrt{2}\pi}, -\frac{\sqrt{2}\bar{\beta}}{\pi}\right\} e^{3i\tau} + \left\{\frac{\bar{\alpha}}{\sqrt{2}\pi}, \frac{i\bar{\alpha}}{\sqrt{2}\pi}, -\frac{\sqrt{2}\beta}{\pi}\right\} e^{-3i\tau} \tag{2.72}$$

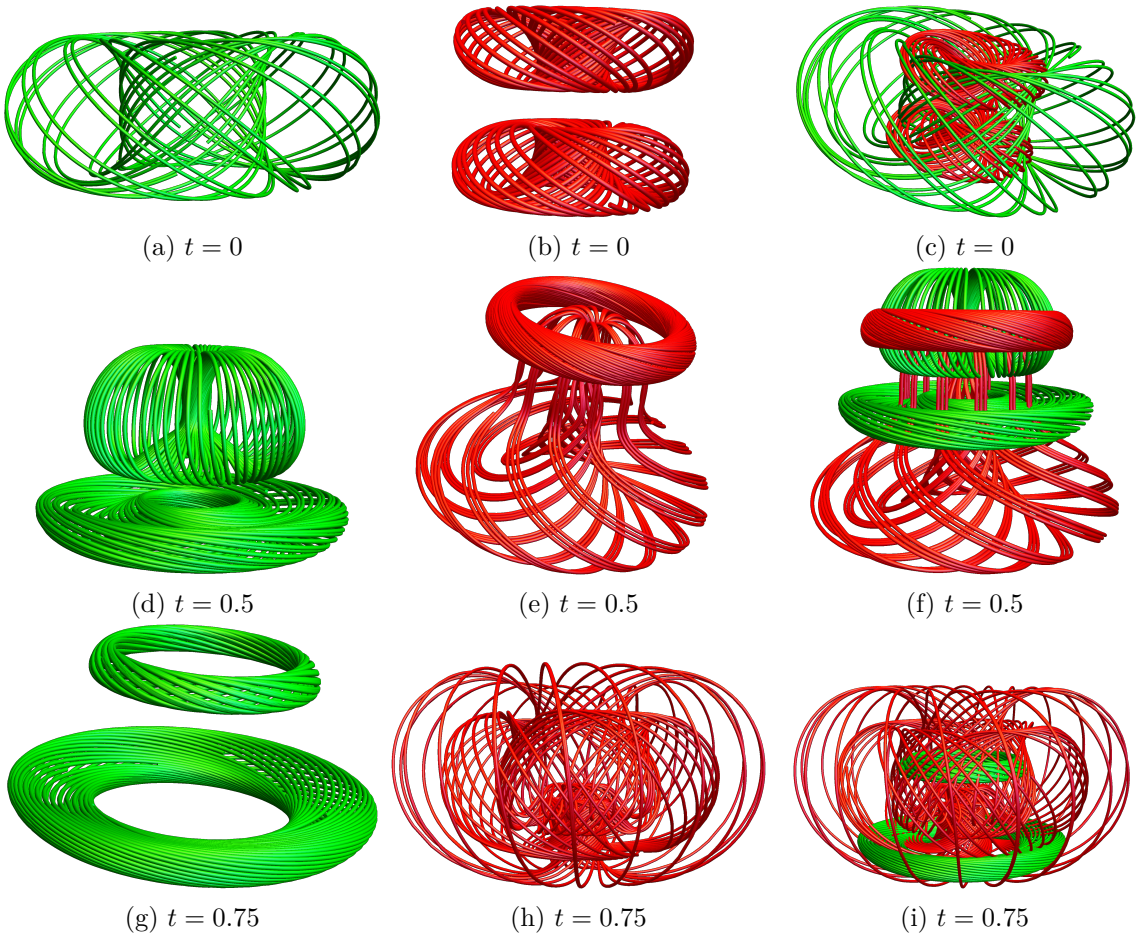

(a) $t = 0$ (b) $t = 0$ (c) $t = 0$

(d) $t = 0.5$ (e) $t = 0.5$ (f) $t = 0.5$

(g) $t = 0.75$ (h) $t = 0.75$ (i) $t = 0.75$

Figure 5: Electric ((a),(d),(g)), magnetic ((b),(e),(h)) and electromagnetic ((c),(f),(i)) field line configurations for a $\{\frac{1}{2}, \frac{1}{2}, -\frac{1}{2}\}$ solution at 3 different times

These solutions seem to mainly consist of disjoint torus knots forming interesting structures when viewed as an electromagnetic field. The magnetic field lines in (Figure 5 (h)) own similar structures as the Hopf fibration. Again the evolution of the field lines in time differs far from a smooth conformal deformation as it was the case in the last example.

As a final example that differs highly from a simple torus knot structure, we consider a solution with $j = \frac{3}{2}$ given by

$$\{\frac{3}{2},-\frac{1}{2},-\frac{3}{2}\} : \frac{1}{2\mathrm{i}}(\left\{ \frac{\sqrt{6}\bar{\alpha}(\bar{\alpha}\alpha - 2\bar{\beta}\beta)}{\pi}, -\frac{\mathrm{i}\sqrt{6}\bar{\alpha}(\bar{\alpha}\alpha - 2\bar{\beta}\beta)}{\pi}, -\frac{2\sqrt{6}\bar{\alpha}^2\bar{\beta}}{\pi} \right\} e^{5\mathrm{i}\tau} \\ - \left\{ \frac{\sqrt{6}\alpha(\bar{\alpha}\alpha - 2\bar{\beta}\beta)}{\pi}, \frac{\mathrm{i}\sqrt{6}\alpha(\bar{\alpha}\alpha - 2\bar{\beta}\beta)}{\pi}, -\frac{2\sqrt{6}\alpha^2\beta}{\pi} \right\} e^{-5\mathrm{i}\tau}) \tag{2.73}$$

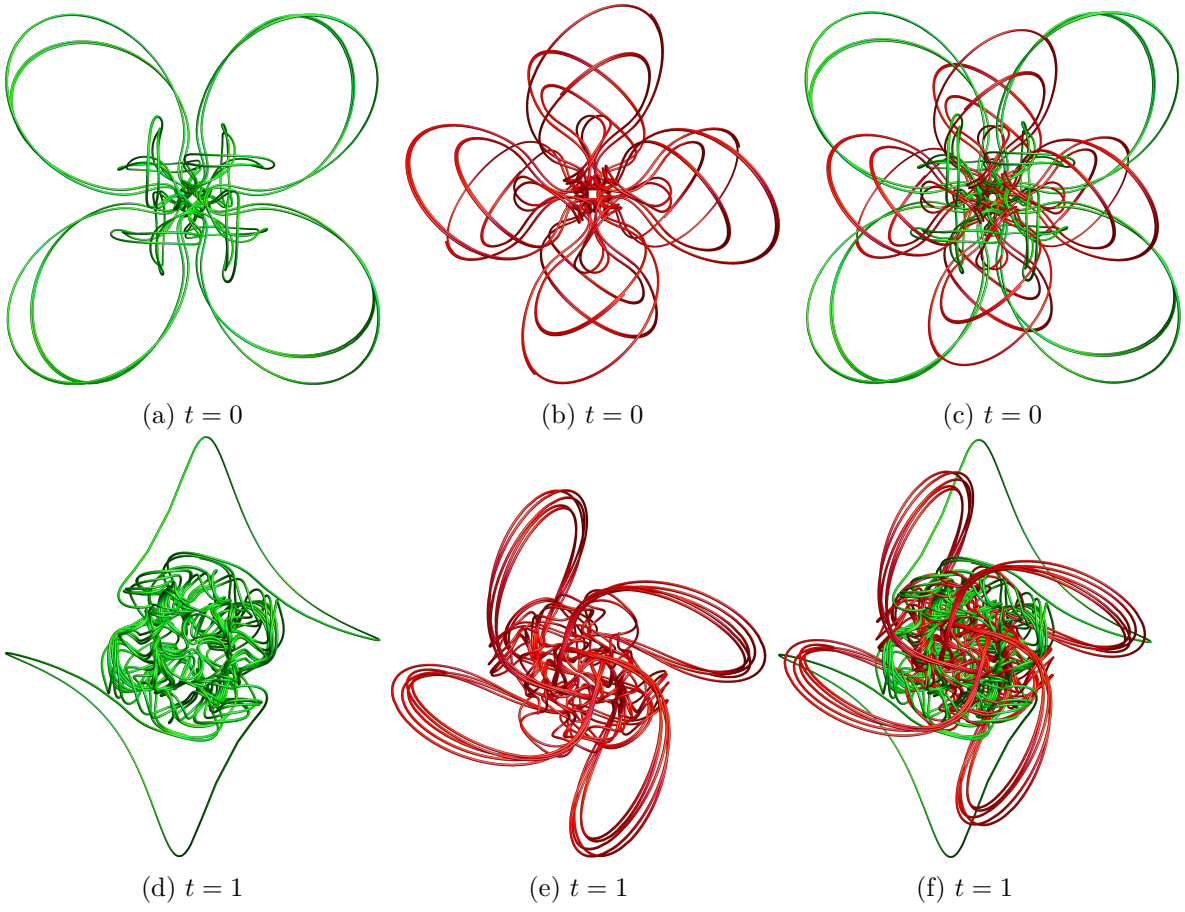

(a) $t = 0$ (b) $t = 0$ (c) $t = 0$

(d) $t = 1$ (e) $t = 1$ (f) $t = 1$

Figure 6: Electric ((a),(d)), magnetic ((b),(e)) and electromagnetic ((c),(f)) field line configurations for a $\{\frac{3}{2},-\frac{1}{2},-\frac{3}{2}\}$ solution at two different times

3 Energy and helicity

Two important quantities missing in the description of electromagnetic knot solutions on $2\mathcal{I} \times \mathbb{S}^3$ till now are the total energy and the electromagnetic helicity, usually given in Minkowski space by the expressions

$$E = \frac{1}{2}\int_{\mathbb{R}^3} \mathrm{d}^3x(\vec{E}^2 + \vec{B}^2) \quad \text{and} \quad h = \frac{1}{2}\int_{\mathbb{R}^3}(A \wedge F + A_D \wedge F_D), \tag{3.1}$$

where A_D and F_D denote the dual gauge potential and dual field strength tensor. As was mentioned before, they can be obtained for the analogue de Sitter quantities via a phase shift of $|\Omega^j|\tau$ by $\frac{\pi}{2}$ for type I or $-\frac{\pi}{2}$ for type II solutions respectively. Both quantities are conserved under conformal transformations for massless fields, thats why we can likewise compute them on de Sitter space. Moreover, they are conserved in time, therefore a neat trick for this manner works by restricting to the $\tau = t = 0$ slice. Thus we are left with an integral over $\mathbb{S}^3$, which simplifies things due to orthogonality properties of the basis of hyperspherical harmonics. By comparing the sphere-framed fields

$$\mathcal{F} = \mathcal{E}_a e^0 \wedge e^a + \frac{1}{2}\epsilon_{abc}\mathcal{B}_a e^b \wedge e^c \tag{3.2}$$

with the Minkowskian fields

$$F = E_i \mathrm{d}x^0 \wedge \mathrm{d}x^i + \frac{1}{2}\epsilon_{ijk}B_i \mathrm{d}x^j \wedge \mathrm{d}x^k \tag{3.3}$$

on this specific slice, the following expression for the energy on $\mathbb{S}^3$ can be derived (Appendix 6.1.2)

$$E = \int_{\mathbb{R}^3} \mathrm{d}^3x(\vec{E}^2 + \vec{B}^2) = \frac{1}{l}\int_{\mathbb{S}^3} \mathrm{d}^3\Omega_3(1 - \omega_4)(\mathcal{E}_a\mathcal{E}_a + \mathcal{B}_a\mathcal{B}_a). \tag{3.4}$$

This defines a quite simple way to compute energies of individual solutions. Note that the ω_4-term drops out of the integration due to orthogonality properties of the basis of hyperspherical harmonics.

For the helicity, we may directly insert $\mathcal{A}$, $\mathcal{A}_D$, $\mathcal{F}$, $\mathcal{F}_D$ into the formula because the metric does not enter. Therefore we obtain

$$\begin{aligned} \mathcal{A} \wedge \mathcal{F} &= X_\alpha e^\alpha \wedge (\mathcal{F}_{0a}e^0 \wedge e^a + \mathcal{F}_{bc}e^b \wedge e^c) \\ &= X_a \mathcal{F}_{bc} e^a \wedge e^b \wedge e^c \\ &= X_a \epsilon^\alpha_{bc}\mathcal{B}_\alpha e^a \wedge e^b \wedge e^c \\ &= 2X_a \mathcal{B}_a \mathrm{d}^3\Omega_3 \end{aligned} \tag{3.5}$$

and can integrate freely over a given spatial slice of $2\mathcal{I} \times \mathbb{S}^3$. For the dual term, note that $\mathcal{F}^D_{bc}$ contains the electric fields $\mathcal{E}_a$. It yields

$$\begin{aligned} \mathcal{A}_D \wedge \mathcal{F}_D &= X^D_a \mathcal{F}^D_{bc} e^a \wedge e^b \wedge e^c \\ &= X^D_a \epsilon^\alpha_{bc}\mathcal{E}_\alpha e^a \wedge e^b \wedge e^c \\ &= 2X^D_a \mathcal{E}_a \mathrm{d}^3\Omega_3. \end{aligned} \tag{3.6}$$

The electromagnetic helicity is then given on $\mathbb{S}^3$ via the expression

$$h = \int_{\mathbb{S}^3} \mathrm{d}^3\Omega_3 (X_a \mathcal{B}_a + X_a^D \mathcal{E}_a). \tag{3.7}$$

In general the energy of a superposition of solutions does not correspond to the sum of their individual energies. Imagine, having two solutions S_I and S_{II} with individual energies $E(S_I)$ and $E(S_{II})$. If we note that the total energy can also be expressed in terms of the norm of the Riemann-Silberstein vector as

$$E = ||\vec{F}||^2 = \frac{1}{2}\int_{\mathbb{R}^3} \mathrm{d}^3x (\vec{F}^* \cdot \vec{F}), \tag{3.8}$$

then the energy of a superposition of both solutions would read

$$E(S_I + S_{II}) = \frac{1}{2}\int_{\mathbb{R}^3} \mathrm{d}^3x ((\vec{F_I} + \vec{F_{II}})^* \cdot (\vec{F_I} + \vec{F_{II}})) \tag{3.9}$$

$$= \frac{1}{2}\int_{\mathbb{R}^3} \mathrm{d}^3x (\vec{F_I}^* \vec{F_I} + \vec{F_{II}}^* \vec{F_{II}} + \vec{F_I}^* \vec{F_{II}} + \vec{F_{II}}^* \vec{F_I}) \tag{3.10}$$

$$\neq E(S_I) + E(S_{II}), \tag{3.11}$$

introducing additional mixed terms. Luckily, it turns out, that the energy for general superpositions of solutions restricted to the $t = \tau = 0$-slice , will result in quite simple expressions.

3.1 General relation between energy and helicity

Energy and helicity are related, as was mentioned in [1] for type I solutions with fixed j and $m = n = 0$. There, a linear relation between both quantities given by

$$E_{\mathrm{I}}^{(j,0,0)} = \frac{2(j+1)}{l} h_{\mathrm{I}}^{(j,0,0)} \tag{3.12}$$

was observed for such solutions. In this chapter, a relation between energy and helicity will be formulated for all possible solutions. For this task, it is very useful to work with the general formalism (2.49), that was introduced earlier instead of working with the complex basis solutions. At first the time dependence will still be shown and later the solutions will be evaluated on the $t = \tau = 0$ slice. It will be enough to compare the corresponding energy and helicity densities

$$l\rho_E = \mathcal{E}_a \mathcal{E}_a + \mathcal{B}_a \mathcal{B}_a, \tag{3.13}$$

$$\rho_h = X_a^D \mathcal{E}_a + X_a \mathcal{B}_a. \tag{3.14}$$

Every electric field (2.30), for any kind of type I and type II solutions with fixed j is given by

$$\mathcal{E}_a = -\dot{X}_a = -\mathrm{i}\Omega_j c_a e^{\mathrm{i}\Omega_j \tau} + \mathrm{i}\Omega_j c_a^* e^{-\mathrm{i}\Omega_j \tau}. \tag{3.15}$$

We then obtain

$$X_a^D \mathcal{E}_a = \pm\Omega_j c_a c_a e^{2\mathrm{i}\Omega_j \tau} \mp 2\Omega_j c_a c_a^* \pm \Omega_j c_a^* c_a^* e^{-2\mathrm{i}\Omega_j \tau}, \tag{3.16}$$

$$\mathcal{E}_a \mathcal{E}_a = -\Omega_j^2 c_a c_a e^{2\mathrm{i}\Omega_j \tau} + 2\Omega_j^2 c_a c_a^* - \Omega_j^2 c_a^* c_a^* e^{-2\mathrm{i}\Omega_j \tau}. \tag{3.17}$$

The equations of motion (2.36) for X_a can be rewritten such that

$$\epsilon_{abc}R_bX_c = \frac{1}{2}\ddot{X}_a + 2(J^2+1)X_a. \tag{3.18}$$

For all magnetic fields for type I and type II solutions it hence yields

$$\mathcal{B}_a = \epsilon_{abc}R_bX_c - 2X_a = \frac{1}{2}\ddot{X}_a + 2J^2X_a, \tag{3.19}$$

allowing for a much more convenient computation of the sphere-framed magnetic fields with the formalism being used. It then follows that

$$\begin{aligned}\mathcal{B}_a &= \frac{1}{2}(-\Omega_j^2 c_a e^{\mathrm{i}\Omega_j\tau} - \Omega_j^2 c_a^* e^{-\mathrm{i}\Omega_j\tau}) + 2j(j+1)(c_a e^{\mathrm{i}\Omega_j\tau} + c_a^* e^{-\mathrm{i}\Omega_j\tau}) \\ &= \mp\Omega_j c_a e^{\mathrm{i}\Omega_j\tau} \mp \Omega_j c_a^* e^{-\mathrm{i}\Omega_j\tau}\end{aligned} \tag{3.20}$$

and we thus obtain the expressions

$$X_a\mathcal{B}_a = \mp\Omega_j c_a c_a e^{2\mathrm{i}\Omega_j\tau} \mp 2\Omega_j c_a c_a^* \mp \Omega_j c_a^* c_a^* e^{-2\mathrm{i}\Omega_j\tau}, \tag{3.21}$$

$$\mathcal{B}_a\mathcal{B}_a = \Omega_j^2 c_a c_a e^{2\mathrm{i}\Omega_j\tau} + 2\Omega_j^2 c_a c_a^* + \Omega_j^2 c_a^* c_a^* e^{-2\mathrm{i}\Omega_j\tau}. \tag{3.22}$$

Finally the energy and helicity densities follow as

$$l\rho_E = 4\Omega_j^2 c_a c_a^*|_{t=0}, \tag{3.23}$$

$$\rho_h = \mp 4\Omega_j c_a c_a^*|_{t=0}. \tag{3.24}$$

This leads to a general relation between energy and helicity given by

$$E = \mp\frac{\Omega_j}{l}h = \begin{cases} \frac{2(j+1)}{l}h & \text{type I} \\ -\frac{2j}{l}h & \text{type II.}\end{cases} \tag{3.25}$$

The relation between energy and helicity was thus proven for every possible solution. The computation for each quantity is fairly simple, hence it shows that these quantities are easily accessible for every kind of solution, which counts as another benefit of this construction method.

As an aside,

$$\dot{h}_m = \int_{\mathbb{S}^3} 2(\mp\mathrm{i}\Omega_j^2 c_a c_a e^{2\mathrm{i}\Omega_j\tau} \pm \mathrm{i}\Omega_j^2 c_a^* c_a^* e^{-2\mathrm{i}\Omega_j\tau})\Big|_{t=\tau=0}\mathrm{d}\Omega^3 = \int_{\mathbb{S}^3} -2(\mathcal{E}_a\mathcal{B}_a)\mathrm{d}^3\Omega_3, \tag{3.26}$$

$$\dot{h}_e = \int_{\mathbb{S}^3} 2(\pm\mathrm{i}\Omega_j^2 c_a c_a e^{2\mathrm{i}\Omega_j\tau} \mp \mathrm{i}\Omega_j^2 c_a^* c_a^* e^{-2\mathrm{i}\Omega_j\tau})\Big|_{t=\tau=0}\mathrm{d}\Omega^3 = \int_{\mathbb{S}^3} 2(\mathcal{E}_a\mathcal{B}_a)\mathrm{d}^3\Omega_3 \tag{3.27}$$

shows that (1.3) and (1.4) are recovered on $2\mathcal{I}\times\mathbb{S}^3$ and that both individual helicities are constant in time for $\mathcal{E}_a\mathcal{B}_a = 0$. This familiar condition leads us over to the next chapter, where all null fields that are contained in this theory are classified.

4 Null fields

In this chapter, null fields on $2\mathcal{I} \times \mathbb{S}^3$ are studied for general superpositions of type I and type II solutions. After obtaining a suitable null condition, the interesting question arises, what structure these fields define. It turns out, that they are deeply related to conics and quadric cones in $\mathbb{CP}^3$, so in order to answer this question, we will need to briefly introduce some formalism from algebraic geometry.

Let $g_{\mathbb{R}^{1,3}}(\cdot,\cdot)$ denote the metric on Minkowski space and $g_{\mathcal{I}\times\mathbb{S}^3}(\cdot,\cdot)$ the metric on de Sitter space. The known null condition in Minkowski space can directly be translated to de Sitter space, because their metrics only differ by some conformal factor λ and in chapter 2, we derived a direct correspondence between F and $\mathcal{F}$ so that

$$g_{\mathbb{R}^{1,3}}(F,F) = \lambda g_{\mathcal{I}\times\mathbb{S}^3}(\mathcal{F},\mathcal{F}) = g_{\mathbb{R}^{1,3}}(F,\star F) = \lambda g_{\mathcal{I}\times\mathbb{S}^3}(\mathcal{F},\star\mathcal{F}) = 0. \tag{4.1}$$

Following that, the null condition on de Sitter space can be compactly written in terms of the Riemann-Silberstein vector as

$$F \cdot F = 0. \tag{4.2}$$

At first, we compute the Riemann-Silberstein vector on de Sitter space for both type I and type II solutions

$$\begin{aligned} F = \mathcal{E}_a + \mathrm{i}\mathcal{B}_a &= -\mathrm{i}\Omega_j c_a e^{\mathrm{i}\Omega_j\tau} + \mathrm{i}\Omega_j c_a^* e^{-\mathrm{i}\Omega_j\tau} \mp \mathrm{i}\Omega_j c_a e^{\mathrm{i}\Omega_j\tau} \mp \mathrm{i}\Omega_j c_a^* e^{-\mathrm{i}\Omega_j\tau} \\ &= \begin{cases} -2\mathrm{i}\Omega_j c_a e^{\mathrm{i}\Omega_j\tau}, & \text{type I} \\ 2\mathrm{i}\Omega_j c_a^* e^{-\mathrm{i}\Omega_j\tau}, & \text{type II} \end{cases}. \end{aligned} \tag{4.3}$$

Substituting this into (4.2), we obtain

$$F \cdot F = \begin{cases} -4\Omega_j^2 c_a c_a e^{2\mathrm{i}\Omega_j\tau}, & \text{type I} \\ -4\Omega_j^2 c_a^* c_a^* e^{-2\mathrm{i}\Omega_j\tau}, & \text{type II} \end{cases} \tag{4.4}$$

what results in two compact null conditions on $2\mathcal{I} \times \mathbb{S}^3$ given by

$$F \cdot F = 0 \Leftrightarrow \begin{cases} \sum_a c_a c_a = 0, & \text{type I} \\ \sum_a c_a^* c_a^* = 0, & \text{type II} \end{cases} \tag{4.5}$$

Every de Sitter field that satisfies (4.5) is classified as a null field and due to (4.1) the null property still holds when transformed to Minkowski space. The following discussion is done for type I solutions, while type II solutions will be discussed later.

Compactly written, the space of null fields is defined as

$$\mathcal{N}_j := \{X_a = c_a e^{\mathrm{i}\Omega_j\tau} + c_a^* e^{-\mathrm{i}\Omega_j\tau} \mid \sum_a c_a c_a = 0 \ \text{ with } \ c_a = \sum_{m,n} c_{mn} Z_a^{mn}\}. \tag{4.6}$$

We can observe that for

$$c_a c_a = \sum_{m,n,m',n'} c_{mn} c_{m'n'} Z_a^{mn} Z_a^{m'n'}, \tag{4.7}$$

there is a summand for every combination of

$$\alpha^k \bar{\alpha}^l \beta^m \bar{\beta}^n \quad \text{with} \quad k+l+m+n = 4j, \tag{4.8}$$

what results in a sum of

$$\frac{(4j+3)!}{3!(4j)!} = \frac{1}{6}(4j+1)(4j+2)(4j+3)$$

terms. These terms are all linearly independent, so they can be formed into a system of linear equations solely depending on the complex coefficients. The main task will be to find solutions to this system of equations. It can also be observed that $c_{mn} \in \mathbb{C}^{(2j+1)(2j+3)}$ for fixed j, so the null condition will generally result in a overdetermined system of equations, but as we will see on the following examples, these systems of equations can be reduced to a smaller number of geometric interesting equations in $\mathbb{CP}^3$. A routine written in Mathematica, that was used for computing and solving those equations for more complex cases is shown in (Appendix 6.2.3).
It will be necessary to give a brief introduction into the terminology of complex algebraic varieties that define conic sections. As a reference for this, [17] was used and contains many further information about this topic.

4.1 Conics and quadric cones

The n-dimensional complex projective space $\mathbb{CP}^n$ is defined as the set of lines through the origin of $\mathbb{C}^{n+1}$

$$\mathbb{CP}^n := \frac{\mathbb{C}^{n+1} \setminus \{0\}}{\sim}, \tag{4.9}$$

where $\sim$ is an equivalence relation of complex points in the same line that passes through the origin given by

$$(x_0, \ldots, x_n) \sim (x'_0, \ldots, x'_n) \Leftrightarrow (x_0, \ldots, x_n) = \lambda(x'_0, \ldots, x'_n) \text{ for } \lambda \in \mathbb{C} \setminus \{0\}. \tag{4.10}$$

$\mathbb{CP}^n$ is equipped with homogeneous coordinates denoted as $[x_0 : x_1 : \cdots : x_n]$ that lie on the same line.

A complex projective variety is defined as a subset in $\mathbb{CP}^n$ that is given by finitely many homogeneous polynomial equations

$$F_1(x_0, \ldots, x_n) = F_2(x_0, \ldots, x_n) = \cdots = F_m(x_0, \ldots, x_n) = 0. \tag{4.11}$$

A subset of a projective variety S is called closed projective subvariety, if it is cut out from S by finitely many homogeneous polynomial equations with complex coefficients and is called irreducible if it is not a union of two different projective closed subvarieties .

Given an irreducible projective variety S in $\mathbb{CP}^2$

$$\begin{aligned} &Ax^2 + Bxy + Cy^2 + Dxz + Eyz + Fz^2 = 0 \\ &\text{with } (A, B, C, D, E, F) \neq (0, 0, 0, 0, 0, 0) \end{aligned} \tag{4.12}$$

together with projective coordinates $[x : y : z]$, S is (up to projective transformations) given by $y^2 = xz$. Those curves are usually called conics and their higher dimensional analogues are called quadric surfaces.

Given an irreducible projective variety S in $\mathbb{CP}^3$

$$\begin{aligned} &Ax^2 + Bxy + Cy^2 + Dxz + Eyz + Fz^2 + Gxw + Hyw + Izw + Kw^2 = 0 \\ &\text{with } (A, B, C, D, E, F, G, H, I, K) \neq (0, 0, 0, 0, 0, 0, 0, 0, 0, 0) \end{aligned} \tag{4.13}$$

together with projective coordinates $[x : y : z : w]$, S is (up to projective translations) either given by a conic $xy = zw$ or by a quadric cone $x^2 = yz$.

$\mathbb{C}^n$ can be identified with $[x_0 : \cdots : x_n] \in \mathbb{CP}^n$ via the injective map

$$(z_1, \ldots, z_n) \mapsto [1 : z_1 : \cdots : z_n] \in \mathbb{CP}^n. \tag{4.14}$$

4.2 Null condition for $j = 0$ solutions

The goal is to derive general solutions for (4.5) and in order to do this, let us first study three examples given by $j = 0$, $j = \frac{1}{2}$ and $j = 1$ with increasing complexity and then try to generalize the results for arbitrary spin. The simplest examples are again the $j = 0$ solutions. In this case, the hyperspherical harmonics have the really simple form

$$Z^{0n}_{a=\{+,3,-\}} = \frac{1}{\sqrt{2}\pi} \begin{array}{c} \begin{array}{ccc} + & 3 & - \end{array} \\ \begin{pmatrix} 1 & 0 & 0 \\ 0 & 1 & 0 \\ 0 & 0 & -1 \end{pmatrix} \end{array} \begin{array}{l} \text{n=-1} \\ \text{n=0} \\ \text{n=1} \end{array} , \tag{4.15}$$

$$Z^{0n}_{a=\{1,2,3\}} = \frac{1}{2\pi} \begin{array}{c} \begin{array}{ccc} 1 & 2 & 3 \end{array} \\ \begin{pmatrix} 1 & -\mathrm{i} & 0 \\ 0 & 0 & \sqrt{2} \\ -1 & -\mathrm{i} & 0 \end{pmatrix} \end{array} \begin{array}{l} \text{n=-1} \\ \text{n=0} \\ \text{n=1} \end{array} . \tag{4.16}$$

The null field condition then reads

$$\begin{cases} c^2_{0,-1} + c^2_{0,0} + c^2_{0,1} = 0 & a = \{+, 3, -\} \\ c^2_{0,0} = 2c_{0,-1}c_{0,1} & a = \{1, 2, 3\} \end{cases} . \tag{4.17}$$

With the freedom of scaling the complex coefficients, we can define coordinates

$$[c_{0,-1} : c_{0,0} : c_{0,1}]$$

and both equations define topological equivalent conics in $\mathbb{CP}^2$ or quadric cones when extended to $\mathbb{CP}^3$. From now on, we will only work on solutions in the $\{1, 2, 3\}$ basis.

One could think of doing this analysis likewise in Minkowski space. As an example, that the null condition in this form can be recovered in Minkowski space, a superposition of $j = 0$ type I solutions

$$\begin{aligned} X_1 &= \frac{1}{2\pi}((c_{0,-1} - c_{0,1})e^{2\mathrm{i}\tau} + (c^*_{0,-1} - c^*_{0,1})e^{-2\mathrm{i}\tau}), \\ X_2 &= -\frac{\mathrm{i}}{\sqrt{2}\pi}((c_{0,-1} + c_{0,1})e^{2\mathrm{i}\tau} - (c^*_{0,-1} + c^*_{0,1})e^{-2\mathrm{i}\tau}), \\ X_3 &= \frac{1}{\sqrt{2}\pi}(c_{0,0}e^{2\mathrm{i}\tau} + c^*_{0,0}e^{-2\mathrm{i}\tau}) \end{aligned} \tag{4.18}$$

can be transformed to Minkowski space in order to compute $\vec{F} \cdot \vec{F} = 0$. With the routine that is shown in (Appendix 6.2.1), it follows that

Out[ ]= $\frac{\mathtt{l}\,(\mathtt{c[0,\ 0]}^2 - 2\,\mathtt{c[0,\ -1]} \times \mathtt{c[0,\ 1]})}{(\mathtt{l} - i\,\mathtt{t})^2 + \mathtt{x}^2 + \mathtt{y}^2 + \mathtt{z}^2} == 0$,

what exactly yields (4.17). For more complex solutions, this method is not very useful because it demands more computational power as deriving solutions on de Sitter space.

4.3 Null condition for $j = \frac{1}{2}$ solutions

We will repeat this procedure for the second simplest case of $j = \frac{1}{2}$ solutions. The hyperspherical harmonics in both basis read

$$Z_+^{mn} = \frac{1}{\pi} \begin{pmatrix} -\sqrt{3}\bar{\alpha} & -\beta & 0 & 0 \\ -\sqrt{3}\bar{\beta} & \alpha & 0 & 0 \end{pmatrix} , \tag{4.19}$$

$$Z_-^{mn} = \frac{1}{\pi} \begin{pmatrix} 0 & 0 & \bar{\alpha} & \sqrt{3}\beta \\ 0 & 0 & \bar{\beta} & -\sqrt{3}\alpha \end{pmatrix} , \tag{4.20}$$

$$Z_1^{mn} = \frac{1}{\sqrt{2}\pi} \begin{pmatrix} -\sqrt{3}\bar{\alpha} & -\beta & \bar{\alpha} & \sqrt{3}\beta \\ -\sqrt{3}\bar{\beta} & \alpha & \bar{\beta} & -\sqrt{3}\alpha \end{pmatrix} , \tag{4.21}$$

$$Z_2^{mn} = \frac{1}{\sqrt{2}\mathrm{i}\pi} \begin{pmatrix} -\sqrt{3}\bar{\alpha} & -\beta & -\bar{\alpha} & -\sqrt{3}\beta \\ -\sqrt{3}\bar{\beta} & \alpha & -\bar{\beta} & \sqrt{3}\alpha \end{pmatrix} , \tag{4.22}$$

$$Z_3^{mn} = \frac{1}{\pi} \begin{pmatrix} 0 & -\sqrt{2}\bar{\alpha} & -\sqrt{2}\beta & 0 \\ 0 & -\sqrt{2}\bar{\beta} & \sqrt{2}\alpha & 0 \end{pmatrix} . \tag{4.23}$$

Employing the notation $m = \{-, +\}$ and $n = \{--, -, +, ++\}$ from now on, we obtain the following coefficients

$$\begin{aligned} c_1 = {} & \frac{1}{\sqrt{2}\pi}(\alpha(c_{+,-} - \sqrt{3}c_{+,++}) + \bar{\alpha}(c_{-,+} - \sqrt{3}c_{-,--}) \\ & + \beta(-c_{-,-} + \sqrt{3}c_{-,++}) + \bar{\beta}(c_{+,+} - \sqrt{3}c_{+,--}), \end{aligned} \tag{4.24}$$

$$\begin{aligned} c_2 = {} & \frac{\mathrm{i}}{\sqrt{2}\pi}(\alpha(-c_{+,-} - \sqrt{3}c_{+,++}) + \bar{\alpha}(c_{-,+} + \sqrt{3}c_{-,--}) \\ & + \beta(c_{-,-} + \sqrt{3}c_{-,++}) + \bar{\beta}(c_{+,+} + \sqrt{3}c_{+,--}), \end{aligned} \tag{4.25}$$

$$c_3 = \frac{\sqrt{2}}{\pi}(\alpha c_{+,+} - \bar{\alpha}c_{-,-} - \beta c_{-,+} - \bar{\beta}c_{+,-}). \tag{4.26}$$

It can be observed, that $c_a c^a = 0$ contains 10 linearly independent terms which can be treated separately. Thus we are left with the following system of equations

$$\begin{aligned} & \alpha^2(c_{+,+}^2 - \sqrt{3}c_{+,-}c_{+,++}) = 0, \\ & \bar{\alpha}^2(c_{-,-}^2 - \sqrt{3}c_{-,+}c_{-,--}) = 0, \\ & \beta^2(c_{-,+}^2 - \sqrt{3}c_{-,-}c_{-,++}) = 0, \\ & \bar{\beta}^2(c_{+,-}^2 - \sqrt{3}c_{+,+}c_{+,--}) = 0, \\ & \alpha\beta(-2c_{-,+}c_{+,+} + \sqrt{3}(c_{-,-}c_{+,++} + c_{+,-}c_{-,++})) = 0, \\ & \bar{\alpha}\bar{\beta}(2c_{-,-}c_{+,-} - \sqrt{3}(c_{-,+}c_{+,--} + c_{+,+}c_{-,--})) = 0, \\ & \bar{\alpha}\beta(c_{-,-}c_{-,+} - 3c_{-,--}c_{-,++}) = 0, \\ & \alpha\bar{\beta}(-c_{+,-}c_{+,+} + 3c_{+,--}c_{+,++}) = 0, \\ & \alpha\bar{\alpha}(c_{-,+}c_{+,-} + 3c_{-,--}c_{+,++} - 2c_{-,-}c_{+,+}) = 0, \\ & \beta\bar{\beta}(-c_{-,-}c_{+,+} - 3c_{-,++}c_{+,--} + 2c_{-,+}c_{+,-}) = 0. \end{aligned} \tag{4.27}$$

These are 10 equations for 8 complex variables, so at first this system of equations is overdetermined. Fortunately, we can reduce these equations to a condition solely depending on the complex coefficients and are able to find the following quadric cone equations

$$\begin{aligned} c_{+,+}^2 &= \sqrt{3}c_{+,-}c_{+,++} \ , & c_{-,+}^2 &= \sqrt{3}c_{-,-}c_{-,++} \ , \\ c_{-,-}^2 &= \sqrt{3}c_{-,--}c_{-,+} \ , & c_{+,-}^2 &= \sqrt{3}c_{+,--}c_{+,+} \ , \end{aligned} \tag{4.28}$$

together with a conic in $\mathbb{CP}^3$

$$3c_{-,++}c_{+,--} = c_{-,+}c_{+,-}. \tag{4.29}$$

There are many more possible solutions (cf. Appendix 6.2.3), but (4.28) and (4.29) describe the only solutions, where no coefficient vanishes and therefore can be considered as the most general ones. As the $j = 0$ null condition can be broken down to a single quadric cone in $\mathbb{CP}^3$, the null condition for $j = \frac{1}{2}$ can be seen as an intersection of 4 quadric cones and one conic each contained in $\mathbb{CP}^3$.

4.4 Null condition for $j = 1$ solutions

A final example that is still manageable to compute in a reasonable amount of time is given by $j = 1$ solutions. We will use the routine that can be seen in (Appendix 6.2.3) to compute the 35 linear independent terms for 15 complex variables. Displaying all of them will be quite confusing, but for the purpose of gaining a better understanding about the structure of those equations, the first few ones are displayed below

$$\begin{aligned} &\alpha^4 \left(3c_{1,1}^2 - 2\sqrt{6}c_{1,0}c_{1,2}\right) = 0, \\ &\bar{\alpha}^4 \left(3c_{-1,-1}^2 - 2\sqrt{6}c_{-1,-2}c_{-1,0}\right) = 0, \\ &\beta^4 \left(3c_{-1,1}^2 - 2\sqrt{6}c_{-1,0}c_{-1,2}\right) = 0, \\ &\bar{\beta}^4 \left(3c_{1,-1}^2 - 2\sqrt{6}c_{1,-2}c_{1,0}\right) = 0, \\ &\bar{\alpha}^3\bar{\beta} \left(-4\sqrt{3}c_{-1,0}c_{0,-2} + 6\sqrt{2}c_{-1,-1}c_{0,-1} - 4\sqrt{3}c_{-1,-2}c_{0,0}\right) = 0, \\ &\beta^3\bar{\alpha} \left(\sqrt{6}c_{-1,0}c_{-1,1} - 6c_{-1,-1}c_{-1,2}\right) = 0, \\ &\beta^3\bar{\beta} \left(3\sqrt{2}c_{-1,2}c_{0,-1} + \sqrt{3}(c_{-1,0}c_{0,1} - 2c_{-1,1}c_{0,0})\right) = 0, \\ &\bar{\alpha}^2\bar{\beta}^2 \left(3c_{0,-1}^2 - 2\sqrt{6}c_{0,-2}c_{0,0} - \sqrt{6}c_{-1,0}c_{1,-2} + 3c_{-1,-1}c_{1,-1} - \sqrt{6}c_{-1,-2}c_{1,0}\right) = 0, \\ &\bar{\alpha}\bar{\beta}^3 \left(-2\sqrt{3}c_{0,0}c_{1,-2} + 3\sqrt{2}c_{0,-1}c_{1,-1} - 2\sqrt{3}c_{0,-2}c_{1,0}\right) = 0. \end{aligned}$$

Due to their linear independency, all equations again need to simultaneously vanish to satisfy the null condition. Therefore we are left with many possible solutions to this system, but as in the last example, the focus lies on the most general solution where

no coefficients vanish. This set of solutions consists of 9 quadric cones

$$
\begin{aligned}
c_{1,1}^2 &= 2\sqrt{\frac{3}{2}}c_{1,0}c_{1,2} \ , & c_{0,-1}^2 &= 2\sqrt{\frac{3}{2}}c_{0,0}c_{0,-2} \ , \\
c_{-1,1}^2 &= 2\sqrt{\frac{3}{2}}c_{-1,0}c_{-1,2} \ , & c_{0,0}^2 &= \frac{3}{2}c_{0,-1}c_{0,1} \ , \\
c_{0,1}^2 &= 2\sqrt{\frac{3}{2}}c_{0,0}c_{0,2} \ , & c_{1,-1}^2 &= 2\sqrt{\frac{3}{2}}c_{1,0}c_{1,-2} \ , \\
c_{1,0}^2 &= \frac{3}{2}c_{1,-1}c_{1,1} \ , & c_{-1,-1}^2 &= 2\sqrt{\frac{3}{2}}c_{-1,0}c_{-1,-2} \ , \\
c_{-1,0}^2 &= \frac{3}{2}c_{-1,-1}c_{-1,1}, &&
\end{aligned}
\tag{4.30}
$$

and 2 conics in $\mathbb{CP}^3$

$$
\begin{aligned}
c_{0,1}c_{1,-1} &= 4c_{0,2}c_{1,-2} \ , \\
c_{-1,1}c_{0,-1} &= 4c_{-1,2}c_{0,-2}.
\end{aligned}
\tag{4.31}
$$

4.5 General solutions

In the previous examples, we have found that the null condition leads to several equations that can be topologically identified with quadric cones and conics in $\mathbb{CP}^3$. Now the task is to describe the structure of these equations and generalize the results for arbitrary j. The former can be done by first analyzing which coefficients are connected in the conic and quadric cone equations. For this, let us take a look at the following tableaux, listing all complex coefficients for the previous examples.

	$n=-1$	$n=0$	$n=1$
$m=0$	$c_{0,-1}$ ⟵	$c_{0,0}$ ⟷	⟶ $c_{0,1}$

Tableau for $j=0$ solutions

	$n=--$	$n=-$	$n=+$	$n=++$
$m=-$	$c_{-,--}$ ⟵	$c_{-,-}$ ⟷	⟶ $\mathbf{c_{-,+}}$	⟶ $\mathbf{c_{-,++}}$
$m=+$	$\mathbf{c_{+,--}}$ ⟵	$\mathbf{c_{+,-}}$ ⟷	⟶ $c_{+,+}$	⟶ $c_{+,++}$

Tableau for $j=\frac{1}{2}$ solutions

	$n=-2$	$n=-1$	$n=0$	$n=1$	$n=2$
$m=-1$	$c_{-1,-2}$ ⟵	$c_{-1,-1}$ ⟷	⟶ $c_{-1,0}$ ⟷	⟶ $\mathbf{c_{-1,1}}$	⟶ $\mathbf{c_{-1,2}}$
$m=0$	$\mathbf{c_{0,-2}}$ ⟵	$\mathbf{c_{0,-1}}$ ⟷	⟶ $c_{0,0}$ ⟷	⟶ $\mathbf{c_{0,1}}$	⟶ $\mathbf{c_{0,2}}$
$m=1$	$\mathbf{c_{1,-2}}$ ⟵	$\mathbf{c_{1,-1}}$ ⟷	⟶ $c_{1,0}$ ⟷	⟶ $c_{1,1}$	⟶ $c_{1,2}$

Tableau for $j=1$ solutions

In can be observed, that there is indeed a reoccurring structure. Based on the results, there are $(2j+1)^2$ equations describing a quadric cone

$$c^2_{m,\tilde{n}} = \zeta_{|\tilde{n}|} c_{m,\tilde{n}-1} c_{m,\tilde{n}+1} \quad \text{for} \quad \tilde{n} = -j, \dots, j \tag{4.32}$$

that always connect 3 horizontally neighboured coefficients with a proportionality factor depending on the absolute value of $\tilde{n}$, while the central one is the coefficient being squared. All these central coefficients fill out the blue cells in the tableaux. Also there are $2j$ equations defining a conic

$$c_{m,j} c_{m+1,-j} = \eta c_{m+1,-j-1} c_{m,j+1} \ , \tag{4.33}$$

sharing the same proportionality factor η. The corresponding coefficients are displayed boldly in the tableaux. As a consequence, the null condition can be thought of some kind foliation of $\mathbb{C}^{(2j+2)(2j+3)}$ into an intersection of $(2j+1)^2$ conics and $2j$ quadric cones in $\mathbb{CP}^3$. We can also deduce, that in the four cases

$$k = 4j \vee l = 4j \vee m = 4j \vee n = 4j, \tag{4.34}$$

the corresponding equations for the complex coefficients readily define four quadric cones given by

$$c^2_{\pm j,\pm j} \propto c_{\pm j,\pm j-1} c_{\pm j,\pm j+1}, \tag{4.35}$$

$$c^2_{\pm j,\mp j} \propto c_{\pm j,\mp j-1} c_{\pm j,\mp j+1}, \tag{4.36}$$

without needing to be reduced by using the remaining equations.

Right now, these results are only based on the 3 examples and solving the system of equations for higher spins gets more and more computationally demanding due to the fast growing number of linearly independent equations needed to be solved. Luckily, just computing these equations is a far more easy task, so the results above can be verified by testing if (4.32) and (4.33) solve the associated system of equations. Before doing that, we can still make some major simplifications.

In general, all the coefficients in the blue cells can be eliminated via expressing them in terms of the $2(j+1)$ outer coefficients $c_{m,\pm(j+1)}$ in the orange cells so that

$$c^{2j+2}_{m,\tilde{n}} = \lambda_{|\tilde{n}|} c^{j+1-\tilde{n}}_{m,j-1} c^{j+1+\tilde{n}}_{m,j+1} \Leftrightarrow c_{m,\tilde{n}} = \lambda^{\frac{1}{2(j+1)}}_{|\tilde{n}|} c^{\frac{j+1-\tilde{n}}{2(j+1)}}_{m,j-1} c^{\frac{j+1+\tilde{n}}{2(j+1)}}_{m,j+1} \tag{4.37}$$

holds, while the outer coefficients can be chosen freely. The conic equations then tell us that

$$\frac{c_{m,-j-1}}{c_{m,j+1}} = \frac{c_{m+1,-j-1}}{c_{m+1,j+1}} \tag{4.38}$$

always holds, so there is a linear dependency between the columns and we may choose

$$c_{m,-j-1} = \kappa c_{m,j+1} \quad \text{with} \quad \kappa \in \mathbb{C}. \tag{4.39}$$

Because the outer coefficients can be chosen freely, we employ the following notation

$$c_{m,j+1} = d_m, \tag{4.40}$$
$$c_{m,-j-1} = \kappa d_m \quad \text{with} \quad d_m \in \mathbb{C}. \tag{4.41}$$

For $j = \frac{1}{2}$, we thus obtain the compact expressions

$$\begin{aligned} c_{+,-} &= \sqrt{3} d_+^{\frac{1}{3}} \kappa^{\frac{2}{3}} d_+^{\frac{2}{3}} = \sqrt{3} \kappa^{\frac{2}{3}} d_+, \\ c_{+,+} &= \sqrt{3} d_+^{\frac{2}{3}} \kappa^{\frac{1}{3}} d_+^{\frac{1}{3}} = \sqrt{3} \kappa^{\frac{1}{3}} d_+, \\ c_{-,+} &= \sqrt{3} d_-^{\frac{1}{3}} \kappa^{\frac{2}{3}} d_-^{\frac{2}{3}} = \sqrt{3} \kappa^{\frac{2}{3}} d_-, \\ c_{-,-} &= \sqrt{3} d_-^{\frac{2}{3}} \kappa^{\frac{1}{3}} d_-^{\frac{1}{3}} = \sqrt{3} \kappa^{\frac{1}{3}} d_- \end{aligned} \tag{4.42}$$

and for $j = 1$ correspondingly

$$\begin{aligned} c_{-1,1} &= 2\kappa^{\frac{1}{4}} d_{-1}, & c_{0,1} &= 2\kappa^{\frac{1}{4}} d_0, & c_{1,1} &= 2\kappa^{\frac{1}{4}} d_1, \\ c_{-1,0} &= \sqrt{6} \kappa^{\frac{2}{4}} d_{-1}, & c_{0,0} &= \sqrt{6} \kappa^{\frac{2}{4}} d_0, & c_{1,0} &= \sqrt{6} \kappa^{\frac{2}{4}} d_1, \\ c_{0,-1} &= 2\kappa^{\frac{3}{4}} d_0, & c_{-1,-1} &= 2\kappa^{\frac{3}{4}} d_{-1}, & c_{1,-1} &= 2\kappa^{\frac{3}{4}} d_1. \end{aligned} \tag{4.43}$$

It is therefore reasonable to make the assumption, that the solutions can be written in a general form of

$$c_{m,n} = \sqrt{\binom{2(j+1)}{j+1-n}} \kappa^{\frac{j+1-n}{2(j+1)}} d_m. \tag{4.44}$$

Indeed, this solves the 84 equations for $j = \frac{3}{2}$ and the 165 equations for $j = 2$ as was tested with the routine in (Appendix 6.2.3). Note, that this is not a general proof, but it is very likely that (4.44) should solve the null equations for arbitrary spin.

There are still some things to mention here. (4.44) yields two extreme solutions

$$\kappa = 0 \Rightarrow \text{only} \quad c_{m,j+1} \neq 0, \tag{4.45}$$
$$\kappa \to \infty \Rightarrow \text{only} \quad c_{m,-j-1} \neq 0, \tag{4.46}$$

leading to a solution space $\mathbb{C}^{2j+1}$. The latter can be explained as follows. If $c_{m,-j-1}$ grows infinitely large, then relative to that, $c_{m,j+1}$ approaches 0 which then accordingly affects the remaining coefficients. Also choosing only $c_{m,\pm(j+1)} \neq 0$ still solves the null equations. The factors κ can freely be scaled by the phase

$$\kappa \mapsto e^{2i\pi k_m} \kappa \quad \text{for} \quad k_m = 0, 1, \ldots, 2(j+1), \tag{4.47}$$

where a specific value of k_m can be chosen for each individual row in the tableaux. Hence we can find $(2j+2)^{2j}$ disjoint copies of spaces of solutions corresponding to the possible choices of k_m with the same structure.

The results hold for all type I solutions but can be expanded intuitively to type II solutions via their correspondence through a parity transformation. To give a simple example, let us look at $j = \frac{3}{2}$ type II solutions. The null condition results in

$$\begin{aligned} {c^*_{+,+}}^2 &= \sqrt{3} c^*_{-,+} c^*_{++,+} \ , & {c^*_{-,+}}^2 &= \sqrt{3} c^*_{+,+} c^*_{--.+} \ , \\ {c^*_{-,-}}^2 &= \sqrt{3} c^*_{+,-} c^*_{--,-} \ , & {c^*_{+,-}}^2 &= \sqrt{3} c^*_{-,-} c^*_{++,-} \ , \end{aligned} \tag{4.48}$$

and

$$c^*_{+,-} c^*_{++,+} = c^*_{+,+} c^*_{++,-}. \tag{4.49}$$

That resembles exactly the conic and quadric cone equations obtained for $j = \frac{1}{2}$ type I solutions with an exchanged role of the magnetic quantum numbers m and n. In fact, that is the case for all solutions, hence all null fields for type II solutions are found through linking the general spin j type I solutions for $c_{m,n}$ (4.44) via a parity transformation to spin $j+1$ type II solutions for $c^*_{m,n}$.

Altogether, all possible null fields arising of this construction method for electromagnetic knots were found together with some interesting topological structure linked to those fields. Because all admissible complex coefficients for the null condition are known, it is now a rather simple task to compute the energy and helicity for all null fields based on the results from last chapter.

5 Conclusion

In this thesis, an introduction to the field of electromagnetic knots was given as well as a recent method to generate such knots in Minkowski space was reviewed and explained. The power of this method was demonstrated through several qualitative visualizations for some generated solutions that gave some impressions about the structure of the knots and how drastically it can change in time. Moreover, a general relation between energy and helicity for all solutions including general superpositions was derived. The main result was a classification of all null solutions contained in the set of solutions that can be generated with the shown method. It turned out, that the coefficients that identify a field as a null field are linked to a set of conics and quadric cones each contained in $\mathbb{CP}^3$. The space of solutions for those coefficients satisfying the null condition allows also for some freedom to choose different phases, resulting in the existence of disjoint copies of such spaces with an identical structure.

Following the ideas from [4] and [12], further research about solutions that can be generated with this method could include symmetry transformations of such knots. Here, the classified null solutions could play an important role. They are well suited for a deeper analysis of their transformation behaviour due to their comprehensive evolution in time and well described linked structure. It makes sense to consider symmetry transformations from the de Sitter group $SO(4,1)$ together with conformal transformations, resulting in all symmetries contained in $SO(4,2)$ for this task. It is generally not obvious, what happens if we carry over transformed solutions like these to Minkowski space and they just may yield some interesting results, such as new knotted solutions or a connection between known solutions via specific transformations. An interesting questions arising here, is for which transformations the null property is preserved and when it breaks.

6 Appendix

6.1 Notes on computations

6.1.1 Compact rewriting of Maxwell's equations on $2\mathcal{I} \times \mathbb{S}^3$

In this appendix, a compact rewriting of

$$-\frac{1}{4}\ddot{X}_a = (J^2+1)X_a + \mathrm{i}\epsilon_{abc}J_bX_c \tag{6.1}$$

in terms of $X_\pm$ and X_3 is shown. We will need the relations

$$X_\pm = \frac{1}{\sqrt{2}}(X_1 \pm \mathrm{i}X_2) \quad \text{and} \quad J_\pm = \frac{1}{\sqrt{2}}(J_1 \pm \mathrm{i}J_2). \tag{6.2}$$

The first equation is obtained by the following computation

$$\begin{aligned}
-\frac{1}{4}\ddot{X}_+ &= \frac{1}{\sqrt{2}}((J^2+1)X_1 + \mathrm{i}(J^2+1)X_2 + \mathrm{i}(J_2X_3 - J_3X_2) - (J_3X_1 - J_1X_3)) \\
&= \frac{1}{\sqrt{2}}((J^2+1)(X_1 + \mathrm{i}X_2) + (J_1 + \mathrm{i}J_2)X_3 - J_3(X_1 + \mathrm{i}X_2)) \\
&= (J^2+1)X_+ + J_+X_3 - J_3X_+ \\
&= (J^2 - J_3 + 1)X_+ + J_+X_3.
\end{aligned} \tag{6.3}$$

Completely analogue to this, it follows that

$$\begin{aligned}
-\frac{1}{4}\ddot{X}_- &= \frac{1}{\sqrt{2}}((J^2+1)X_1 - \mathrm{i}(J^2+1)X_2 + \mathrm{i}(J_2X_3 - J_3X_2) + (J_3X_1 - J_1X_3)) \\
&= \frac{1}{\sqrt{2}}((J^2+1)(X_1 - iX_2) + J_3(X_1 - \mathrm{i}X_2) - (J_1 - \mathrm{i}J_2)X_3) \\
&= (J^2+1)X_- + J_3X_- - J_-X_3 \\
&= (J^2 + J_3 + 1)X_- - J_-X_3.
\end{aligned} \tag{6.4}$$

The equation of motion for X_3 can be obtained as follows

$$\begin{aligned}
-\frac{1}{4}\ddot{X}_3 &= (J^2+1)X_3 + \mathrm{i}(J_1X_2 - J_2X_1) \\
&= (J^2+1)X_3 + \frac{1}{2}((J_+ + J_-)(X_+ - X_-) - (J_+ - J_-)(X_+ + X_-)) \\
&= (J^2+1)X_3 - J_+X_- + J_-X_+.
\end{aligned} \tag{6.5}$$

Finally a rewriting of the gauge condition (2.27) is given by

$$\begin{aligned}
0 &= J_1X_1 + J_2X_2 + J_3X_3 \\
&= \frac{1}{2}((J_+ + J_-)(X_+ + X_-) - (J_+ - J_-)(X_+ - X_-)) + J_3X_3 \\
&= J_+X_- + J_-X_+ + J_3X_3.
\end{aligned} \tag{6.6}$$

6.1.2 Computing the energy in spherical coordinates

In this appendix, a derivation of the following formula on the $t = \tau = 0$ -slice is given

$$\int_{\mathbb{R}^3} \mathrm{d}^3x \vec{E}^2 = \frac{1}{l} \int_{\mathbb{S}^3} \mathrm{d}^3\Omega_3 (1 - \omega_4) \mathcal{E}_a \mathcal{E}_a \tag{6.7}$$

$$\int_{\mathbb{R}^3} \mathrm{d}^3x \vec{B}^2 = \frac{1}{l} \int_{\mathbb{S}^3} \mathrm{d}^3\Omega_3 (1 - \omega_4) \mathcal{B}_a \mathcal{B}_a. \tag{6.8}$$

The basis of 1-forms on $\mathbb{S}^3$ evaluated on the given slice read

$$e^0\Big|_{\tau=t=0} = \frac{2l}{r^2 + l^2} \mathrm{d}t \tag{6.9}$$

$$e^a\Big|_{\tau=t=0} = \frac{4l}{(r^2 + l^2)^2} (\frac{1}{2}(l^2 - r^2)\delta^a_k + x^a x^k + l\epsilon^a_{jk} x^j) \mathrm{d}x^k. \tag{6.10}$$

Thus, e^0 depends only on $\mathrm{d}t$ and e^a depends on $\mathrm{d}x^k$. Let us first consider the electric fields. The field strength tensor in Minkowski space is given by

$$F = E_i \mathrm{d}t \wedge \mathrm{d}x^i + \frac{1}{2} \epsilon_{ijk} B_i \mathrm{d}x^j \wedge \mathrm{d}x^k \tag{6.11}$$

and the analogue quantity in de Sitter space reads

$$\mathcal{F} = \mathcal{E}_a e^0 \wedge e^a + \frac{1}{2} \epsilon_{abc} \mathcal{B}_a e^b \wedge e^c. \tag{6.12}$$

By comparison of coefficients for (6.11) and (6.12)

$$E_i \mathrm{d}t \wedge \mathrm{d}x^i = \mathcal{E}_a e^0 \wedge e^a, \tag{6.13}$$

it can be observed that the Minkowskian electric fields can be expressed via

$$E_i = \mathcal{E}_a e^0_t e^a_i, \tag{6.14}$$

with coefficients

$$e^0_t = \frac{2l}{r^2 + l^2} \tag{6.15}$$

$$e^a_i = \frac{4l}{(r^2 + l^2)^2} (\frac{1}{2}(l^2 - r^2)\delta^a_i + x^a x^i + l\epsilon^a_{ji} x^j). \tag{6.16}$$

Then, computing the square of the electric fields yields

$$E_i E_i = \mathcal{E}_a \mathcal{E}_{a'} (e^0_t)^2 e^a_i e^{a'}_i = \frac{16l^4}{(l^2 + r^2)^4} \mathcal{E}_a \mathcal{E}_a. \tag{6.17}$$

We need to transform the spherical volume element

$$\mathrm{d}^3\Omega_3 = e^1 \wedge e^2 \wedge e^3 \tag{6.18}$$

to Minkowski space. Performing the wedge product (6.18) yields

$$\begin{aligned} e^1 \wedge e^2 \wedge e^3 &= \frac{8l^3}{l^2+r^2} \mathrm{d}x^1 \wedge \mathrm{d}x^2 \wedge \mathrm{d}x^3 \\ &= \frac{8l^3}{l^2+r^2} \mathrm{d}^3x. \end{aligned} \tag{6.19}$$

Therefore, we arrive at the relation

$$\begin{aligned} E_i E_i \mathrm{d}^3x &= \frac{l^2+r^2}{8l^3} \frac{16l^4}{(l^2+r^2)^4} \mathcal{E}_a \mathcal{E}_a \mathrm{d}^3\Omega_3 \\ &= \frac{2l}{(l^2+r^2)^3} \mathcal{E}_a \mathcal{E}_a \mathrm{d}^3\Omega_3. \end{aligned} \tag{6.20}$$

Considering

$$w_4\Big|_{t=0} = \frac{r^2-l^2}{r^2+l^2}, \tag{6.21}$$

it then follows that

$$\frac{1}{l} \frac{2l^2}{r^2+l^2} = \frac{1}{l}(1-\omega_4) \tag{6.22}$$

and we are thus able to find the formula

$$\int_{\mathbb{R}^3} \mathrm{d}^3x \vec{E}^2 = \frac{1}{l} \int_{\mathbb{S}^3} \mathrm{d}^3\Omega_3 (1-\omega_4) \mathcal{E}_a \mathcal{E}_a.$$

Going over to the magnetic fields, the whole computation works completely analogue but is a bit more technical demanding. Again, via comparison of coefficients for

$$\frac{1}{2} \epsilon_{abc} \mathcal{B}_a e^b \wedge e^c = \frac{1}{2} B_i \epsilon_{ijk} dx^j \wedge dx^k, \tag{6.23}$$

we can observe that the Minkowskian magnetic fields are given by

$$B_i = \frac{1}{2} \epsilon_{abc} \epsilon_{ijk} e^b_j e^c_k \mathcal{B}_a. \tag{6.24}$$

It then follows that

$$\begin{aligned} B_i B_i &= \frac{1}{4} \epsilon_{abc} \epsilon_{a'b'c'} \mathcal{B}_a \mathcal{B}_{a'} \epsilon_{ijk} \epsilon_{ij'm'} e^b_j e^c_k e^{b'}_{j'} e^{c'}_{k'} \\ &= \frac{1}{2} \epsilon_{abc} \epsilon_{a'b'c'} \mathcal{B}_a \mathcal{B}_{a'} e^b_j e^{b'}_j e^c_k e^{c'}_k. \end{aligned} \tag{6.25}$$

Computing (6.25) yields a similar expression as for the square of the electric fields

$$B_i B_i = \frac{16l^4}{(l^2+r^2)^4} \mathcal{B}_a \mathcal{B}_a. \tag{6.26}$$

Hence analogously to the previous case, the formula

$$\int_{\mathbb{R}^3} \mathrm{d}^3x \vec{B}^2 = \frac{1}{l} \int_{\mathbb{S}^3} \mathrm{d}^3\Omega_3 (1-\omega_4) \mathcal{B}_a \mathcal{B}_a, \tag{6.27}$$

holds.

6.2 Mathematica Code

In the last appendix, some important code that was used for numerous computations in this thesis is presented. For an implementation of exterior differential calculus, the **scalarEDCcode.nb**[1] from Sotirios Bonanos was used. Nearly all functions were defined locally in the routines but of course depending on what one wants to work on in a single notebook, it could come in handy to define some of the functions needed for different computations globally.

6.2.1 Routine for computing the Riemann-Silberstein vector

The routine for computing the Riemann-Silberstein vector for de Sitter configurations X_a is shown below. Because all necessary quantities like $\mathcal{A}$, A as well as the components of $\vec{E}$ and $\vec{B}$ are defined locally in this routine, accessing them can be easily done via **Print**[ ]. It turned out that simplifying each step in the computation works best. For expressions that are not too complicated **RS**[ ]//**FullSimplify** can be used, to further simplify the output. In general, it makes sense to first try the computations without further simplifications.

```
δ[i_, j_] := If[i == j, 1, 0]
ϵ[a_, i_, j_] := If[{a, i, j} == {1, 2, 3} ∨ {a, i, j} == {3, 1, 2} ∨ {a, i, j} == {2, 3, 1}, 1,
  If[{a, i, j} == {3, 2, 1} ∨ {a, i, j} == {1, 3, 2} ∨ {a, i, j} == {2, 1, 3}, -1, 0], 0]
γ := (2 l^2) / (Sqrt[4 l^2 * t^2 + (r^2 - t^2 + l^2)^2])
RS[X1_, X2_, X3_] :=
 {X[1] := X1;
  X[2] := X2;
  X[3] := X3;
  B[0] := t;
  B[1] := x;
  B[2] := y;
  B[3] := z;
  e[a_] := Simplify[(γ^2 / l^3) * t * B[a] × d[t] - Sum[(γ^2 / l^3) * (1 / 2) * (t^2 - r^2 + l^2) δ[a, k] × d[B[k]], {k, 1, 3}] -
     Sum[(γ^2 / l^3) B[a] × B[k] × d[B[k]], {k, 1, 3}] - (γ^2 / l^3) * Sum[l * ϵ[a, j, k] × B[j] × d[B[k]], {j, 1, 3}, {k, 1, 3}]];
  𝒜[a_] := Simplify[X[a] * e[a]];
  FullGauge := reWrite[Sum[𝒜[a], {a, 1, 3}]];
  A[0] := FullGauge /. {d[t] → 1, d[x] → 0, d[y] → 0, d[z] → 0};
  A[1] := FullGauge /. {d[t] → 0, d[x] → 1, d[y] → 0, d[z] → 0};
  A[2] := FullGauge /. {d[t] → 0, d[x] → 0, d[y] → 1, d[z] → 0};
  A[3] := FullGauge /. {d[t] → 0, d[x] → 0, d[y] → 0, d[z] → 1};
  F[u_, v_] := D[A[u], B[v]] - D[A[v], B[u]];
  E1 := F[0, 1] // Simplify;
  E2 := F[0, 2] // Simplify;
  E3 := F[0, 3] // Simplify;
  B1 := F[2, 3] // Simplify;
  B2 := F[3, 1] // Simplify;
  B3 := F[1, 2] // Simplify;
  {E1, E2, E3} + I * {B1, B2, B3} // Simplify}
```

[1] URL: https://library.wolfram.com/infocenter/MathSource/683 (accessed January 22, 2020)

6.2.2 Visualization of field lines

Before being able to visualize field lines for a specific field in Minkowski space, we first need to compute Z_a^{mn} in the $a = \{1, 2, 3\}$ basis. The code below works for a maximum value of $j - m = 3$ what corresponds to type I solutions with $j = 0, \frac{1}{2}, 1, \frac{3}{2}$. In order to compute solutions for higher values of j, one just need to add the corresponding higher order partial derivatives occurring in $Y_{j;m,n}$.

```
Z123[J_, M_, N_] := {
  f[α_] := α^(2 φ);
  g[α_, b_] := (-b / Sqrt[2])^(φ - ν) * D[f[α], {α, (φ - ν)}];
  Y[j_, m_, n_] :=
   If[j - m == 0, Sqrt[(2 j + 1) / (2 Pi^2)] * Sqrt[((2^(j - m)) * (j + m)!) / ((2 j)! * (j - m)!)] *
     Sqrt[((2^(j - n)) * (j + n)!) / ((2 j)! * (j - n)!)] * (g[α, b]),
    If[j - m == 1, Sqrt[(2 j + 1) / (2 Pi^2)] * Sqrt[((2^(j - m)) * (j + m)!) / ((2 j)! * (j - m)!)] *
      Sqrt[((2^(j - n)) * (j + n)!) / ((2 j)! * (j - n)!)] *
      (((a / (Sqrt[2]))) D[g[α, b], {b, 1}] + (-β / Sqrt[2]) D[g[α, b], {α, 1}]),
     If[j - m == 2, Sqrt[(2 j + 1) / (2 Pi^2)] * Sqrt[((2^(j - m)) * (j + m)!) / ((2 j)! * (j - m)!)] *
       Sqrt[((2^(j - n)) * (j + n)!) / ((2 j)! * (j - n)!)] *
       (((a / (Sqrt[2])))^2 D[g[α, b], {b, 2}] + (-β / Sqrt[2])^2 D[g[α, b], {α, 2}] -
         2 (a / (Sqrt[2])) * (β / Sqrt[2]) D[D[g[α, b], α], b]),
      If[j - m == 3, Sqrt[(2 j + 1) / (2 Pi^2)] * Sqrt[((2^(j - m)) * (j + m)!) / ((2 j)! * (j - m)!)] *
        Sqrt[((2^(j - n)) * (j + n)!) / ((2 j)! * (j - n)!)] *
        (((a / (Sqrt[2])))^3 D[g[α, b], {b, 3}] + (-β / Sqrt[2])^3 D[g[α, b], {α, 3}] +
          3 (a / (Sqrt[2])) * (β / Sqrt[2])^2 D[D[g[α, b], b], {α, 2}] -
          3 * (β / Sqrt[2]) * (a / (Sqrt[2]))^2 D[D[g[α, b], α], {b, 2}]), 0]]];
  XPlusI[j_, m_, n_] := Sqrt[((j - n) * (j - n + 1)) / 2] * (Y[j, m, (n + 1)]);
  X3I[j_, m_, n_] := Sqrt[(j + 1)^2 - n^2] Y[j, m, n];
  XMinusI [j_, m_, n_] := -Sqrt[((j + n) (j + n + 1)) / 2] Y[j, m, (n - 1)];
  Z[m_, n_] :=
   FullSimplify[{XPlusI[J, m, n] /. {φ → J, ν → (n + 1)}, XMinusI[J, m, n] /. {φ → J, ν → (n - 1)},
     X3I[J, m, n] /. {φ → J, ν → n}}];
  1 / Sqrt[2] (Z[M, N][[1]] + Z[M, N][[2]]), 1 / (Sqrt[2] * I) (Z[M, N][[1]] - Z[M, N][[2]]),
  Z[M, N][[3]]}
```

Below an example for computing a particular $\{\frac{1}{2}, \frac{1}{2}, -\frac{1}{2}\}$ solution is given.

```
γ := (2 l^2) / (Sqrt[4 l^2 * t^2 + (r^2 - t^2 + l^2)^2])
ω[1] := γ * x / l
ω[2] := γ * y / l
ω[3] := γ * z / l
ω[4] := γ * (r^2 - t^2 - l^2) / (2 l^2)
eiτ[k_] := (((l + I * t)^2 + r^2) / Sqrt[4 l^2 * t^2 + (r^2 - t^2 + l^2)^2])^k
Z123[1 / 2, 1 / 2, -1 / 2]
```

$$\left\{\frac{\alpha}{\sqrt{2}\,\pi}, -\frac{i\,\alpha}{\sqrt{2}\,\pi}, -\frac{\sqrt{2}\,b}{\pi}\right\}$$

```
FullSimplify[(1 / 2 (Z123[1 / 2, 1 / 2, -1 / 2] eiτ[3] + Z123[1 / 2, -1 / 2, 1 / 2] eiτ[-3])) /.
  {α → ω[1] + I * ω[2], β → ω[3] + I * ω[4], a → ω[1] - I * ω[2], b → ω[3] - I * ω[4]}]
```

$$\left\{\left(\sqrt{2}\,l\right.\right.$$
$$\left(l^6 x - 6 l^5 t y + 3 l^4 x \left(-5 t^2 + x^2 + y^2 + z^2\right) + 3 l^2 x \left(-5 t^2 + x^2 + y^2 + z^2\right) \left(-t^2 + x^2 + y^2 + z^2\right) - \right.$$
$$\left.\left.6 l t y \left(-t^2 + x^2 + y^2 + z^2\right)^2 + x \left(-t^2 + x^2 + y^2 + z^2\right)^3 + 4 l^3 t y \left(5 t^2 - 3 \left(x^2 + y^2 + z^2\right)\right)\right)\right) /$$
$$\left(\pi \left((l - i\,t)^2 + x^2 + y^2 + z^2\right)^2 \left((l + i\,t)^2 + x^2 + y^2 + z^2\right)^2\right),\ \left(\sqrt{2}\,l\right.$$
$$\left(6 l^5 t x + l^6 y + 3 l^4 y \left(-5 t^2 + x^2 + y^2 + z^2\right) + 3 l^2 y \left(-5 t^2 + x^2 + y^2 + z^2\right) \left(-t^2 + x^2 + y^2 + z^2\right) + \right.$$
$$\left.\left.6 l t x \left(-t^2 + x^2 + y^2 + z^2\right)^2 + y \left(-t^2 + x^2 + y^2 + z^2\right)^3 + 4 l^3 t x \left(-5 t^2 + 3 \left(x^2 + y^2 + z^2\right)\right)\right)\right) /$$
$$\left(\pi \left((l - i\,t)^2 + x^2 + y^2 + z^2\right)^2 \left((l + i\,t)^2 + x^2 + y^2 + z^2\right)^2\right),$$
$$\left(-\left((l + i\,t)^2 + x^2 + y^2 + z^2\right)^6 \left(2 l z + i \left(l^2 + t^2 - x^2 - y^2 - z^2\right)\right) - \right.$$
$$\left.\left(2 l z - i \left(l^2 + t^2 - x^2 - y^2 - z^2\right)\right) \left(4 l^2 t^2 + \left(l^2 - t^2 + x^2 + y^2 + z^2\right)^2\right)^3\right) /$$
$$\left.\left(\sqrt{2}\,\pi \left((l + i\,t)^2 + x^2 + y^2 + z^2\right)^3 \left(4 l^2 t^2 + \left(l^2 - t^2 + x^2 + y^2 + z^2\right)^2\right)^2\right)\right\}$$

Afterwards, we can use **RS[ ]** to compute the electric and magnetic fields in Minkowski space.

```
RS[
 (Sqrt[2] l (l^6 x - 6 l^5 t y + 3 l^4 x (-5 t^2 + x^2 + y^2 + z^2) + 3 l^2 x (-5 t^2 + x^2 + y^2 + z^2) (-t^2 + x^2 + y^2 + z^2) -
      6 l t y (-t^2 + x^2 + y^2 + z^2)^2 + x (-t^2 + x^2 + y^2 + z^2)^3 + 4 l^3 t y (5 t^2 - 3 (x^2 + y^2 + z^2))))/
  (π ((l - i t)^2 + x^2 + y^2 + z^2)^2 ((l + i t)^2 + x^2 + y^2 + z^2)^2),
 (Sqrt[2] l (6 l^5 t x + l^6 y + 3 l^4 y (-5 t^2 + x^2 + y^2 + z^2) + 3 l^2 y (-5 t^2 + x^2 + y^2 + z^2) (-t^2 + x^2 + y^2 + z^2) +
      6 l t x (-t^2 + x^2 + y^2 + z^2)^2 + y (-t^2 + x^2 + y^2 + z^2)^3 + 4 l^3 t x (-5 t^2 + 3 (x^2 + y^2 + z^2))))/
  (π ((l - i t)^2 + x^2 + y^2 + z^2)^2 ((l + i t)^2 + x^2 + y^2 + z^2)^2),
 (-((l + i t)^2 + x^2 + y^2 + z^2)^6 (2 l z + i (l^2 + t^2 - x^2 - y^2 - z^2)) -
    (2 l z - i (l^2 + t^2 - x^2 - y^2 - z^2)) (4 l^2 t^2 + (l^2 - t^2 + x^2 + y^2 + z^2)^2)^3)/
  (Sqrt[2] π ((l + i t)^2 + x^2 + y^2 + z^2)^3 (4 l^2 t^2 + (l^2 - t^2 + x^2 + y^2 + z^2)^2)^2)]
Out[]= {{1/(π (l^2 - 2 i l t - t^2 + x^2 + y^2 + z^2)^4
   12 Sqrt[2] l^2 (i l^3 (x + 3 i y) + 2 i t^3 y + 2 t^2 x z + 2 l^2 (t x + 2 i t y + 2 x z + 3 i y z) - 2 i t y (x^2 + y^2 + z^2) - 2 x z (x^2 + y^2 + z^2) +
      l (i x^3 + t^2 (-i x - y) + 3 x^2 y + t (-2 i x z + 6 y z) + i x (y^2 - 5 z^2) + 3 y (y^2 + z^2))), 1/(π (l^2 - 2 i l t - t^2 + x^2 + y^2 + z^2)^4
   12 Sqrt[2] l^2 (-2 i t^3 x + l^3 (3 x + i y) + 2 t^2 y z + 2 l^2 (-2 i t x + t y - 3 i x z + 2 y z) + 2 i t x (x^2 + y^2 + z^2) -
      2 y z (x^2 + y^2 + z^2) + l (-3 x^3 + t^2 (x - i y) + i x^2 y - 2 t (3 x + i y) z - 3 x (y^2 + z^2) + i (y^3 - 5 y z^2))),
  (12 Sqrt[2] l^2 (l^4 - t^4 + x^4 + 2 x^2 y^2 + y^4 + 2 t^2 z^2 - z^4 - 2 i l^3 (t + z) - 4 l^2 (x^2 + y^2 + t z) -
      2 i l (t + z) (t^2 - 2 x^2 - 2 y^2 - 2 t z + z^2)))/(π (l^2 - 2 i l t - t^2 + x^2 + y^2 + z^2)^4)}}

EE[l_, t_] :=
 Re[
  {1/(π (l^2 - 2 i l t - t^2 + x^2 + y^2 + z^2)^4) 12 Sqrt[2] l^2
    (i l^3 (x + 3 i y) + 2 i t^3 y + 2 t^2 x z + 2 l^2 (t x + 2 i t y + 2 x z + 3 i y z) - 2 i t y (x^2 + y^2 + z^2) -
      2 x z (x^2 + y^2 + z^2) + l (i x^3 + t^2 (-i x - y) + 3 x^2 y + t (-2 i x z + 6 y z) + i x (y^2 - 5 z^2) + 3 y (y^2 + z^2))),
   1/(π (l^2 - 2 i l t - t^2 + x^2 + y^2 + z^2)^4) 12 Sqrt[2] l^2
    (-2 i t^3 x + l^3 (3 x + i y) + 2 t^2 y z + 2 l^2 (-2 i t x + t y - 3 i x z + 2 y z) + 2 i t x (x^2 + y^2 + z^2) -
      2 y z (x^2 + y^2 + z^2) + l (-3 x^3 + t^2 (x - i y) + i x^2 y - 2 t (3 x + i y) z - 3 x (y^2 + z^2) + i (y^3 - 5 y z^2))),
   (12 Sqrt[2] l^2 (l^4 - t^4 + x^4 + 2 x^2 y^2 + y^4 + 2 t^2 z^2 - z^4 - 2 i l^3 (t + z) - 4 l^2 (x^2 + y^2 + t z) -
      2 i l (t + z) (t^2 - 2 x^2 - 2 y^2 - 2 t z + z^2)))/(π (l^2 - 2 i l t - t^2 + x^2 + y^2 + z^2)^4)}]
BB[l_, t_] :=
 Im[
  {1/(π (l^2 - 2 i l t - t^2 + x^2 + y^2 + z^2)^4) 12 Sqrt[2] l^2
    (i l^3 (x + 3 i y) + 2 i t^3 y + 2 t^2 x z + 2 l^2 (t x + 2 i t y + 2 x z + 3 i y z) - 2 i t y (x^2 + y^2 + z^2) -
      2 x z (x^2 + y^2 + z^2) + l (i x^3 + t^2 (-i x - y) + 3 x^2 y + t (-2 i x z + 6 y z) + i x (y^2 - 5 z^2) + 3 y (y^2 + z^2))),
   1/(π (l^2 - 2 i l t - t^2 + x^2 + y^2 + z^2)^4) 12 Sqrt[2] l^2
    (-2 i t^3 x + l^3 (3 x + i y) + 2 t^2 y z + 2 l^2 (-2 i t x + t y - 3 i x z + 2 y z) + 2 i t x (x^2 + y^2 + z^2) -
      2 y z (x^2 + y^2 + z^2) + l (-3 x^3 + t^2 (x - i y) + i x^2 y - 2 t (3 x + i y) z - 3 x (y^2 + z^2) + i (y^3 - 5 y z^2))),
   (12 Sqrt[2] l^2 (l^4 - t^4 + x^4 + 2 x^2 y^2 + y^4 + 2 t^2 z^2 - z^4 - 2 i l^3 (t + z) - 4 l^2 (x^2 + y^2 + t z) -
      2 i l (t + z) (t^2 - 2 x^2 - 2 y^2 - 2 t z + z^2)))/(π (l^2 - 2 i l t - t^2 + x^2 + y^2 + z^2)^4)}]
```

A fast working routine for computing field lines for the obtained solutions written by Jens Nöckel[2] was used with his consent for the visualizations in this thesis. It is needed to find a suitable value for the Working Precision within **NDSolve**[ ] in order to achieve high numerical precision together with a reasonable computation time.

```
fieldSolve[field_, varlist_, xi0_, tmax_, debug_: False] :=
 Module[{xiVec, equationSet, t},
  If[Length[varlist] ≠ Length[xi0],
   Print["Number of variables must equal number of initial conditions\nUSAGE:\n" <> fieldSolve::usage];
   Abort[]];
  xiVec = Through[varlist[t]];
  (*Below,Simplify[equationSet] would cost extra time and doesn't help with the numerical solution,
  so don't try to simplify.*)
  equationSet = Join[Thread[Map[D[#, t] &, xiVec] == Normalize[field /. Thread[varlist → xiVec]]],
    Thread[(xiVec /. t → 0) == xi0]];
  If[debug,
   Print[Row[{"Numerically solving the system of equations\n\n",
      TraditionalForm[(Simplify[equationSet] /. t → "t") // TableForm]}]]];
  (*This is where the differential equation is solved.The Quiet[] command suppresses warning
   messages because numerical precision isn't crucial for our plotting purposes:*)
  Map[Head, First[xiVec /. Quiet[NDSolve[equationSet, xiVec, {t, 0, tmax}, WorkingPrecision → 30]]], 2]]

fieldLinePlot[field_, varList_, seedList_, opts : OptionsPattern[]] :=
  Module[{sols, localVars, var, localField, plotOptions, tubeFunction, tubePlotStyle, postProcess = {}},
   plotOptions = FilterRules[{opts}, Options[ParametricPlot3D]];
   tubeFunction = OptionValue["TubeFunction"];
   If[tubeFunction =!= None, tubePlotStyle = Cases[OptionValue[PlotStyle], Except[_Tube]];
    plotOptions = FilterRules[plotOptions, Except[{PlotStyle, ColorFunction, ColorFunctionScaling}]];
    postProcess = Line[x_] :> Join[tubePlotStyle, {CapForm["Butt"], Tube[x, tubeFunction @@@ x]}]];
   If[Length[seedList[[1, 1]]] ≠ Length[varList],
    Print["Number of variables must equal number of initial conditions\nUSAGE:\n" <> fieldLinePlot::usage];
    Abort[]];
   localVars = Array[var, Length[varList]];
   localField = ReleaseHold[Hold[field] /. Thread[Map[HoldPattern, Unevaluated[varList]] → localVars]];
   (*Assume that each element of seedList specifies a point AND the length of the field line:*)
   Show[
    ParallelTable[
     ParametricPlot3D[Evaluate[Through[#[t]]], {t, #[[1, 1, 1, 1]], #[[1, 1, 1, 2]]},
         Evaluate@Apply[Sequence, plotOptions]] &[
       fieldSolve[localField, localVars, seedList[[i, 1]], seedList[[i, 2]]]] /. postProcess,
      {i, Length[seedList]}]]];

Options[fieldLinePlot] = Append[Options[ParametricPlot3D], "TubeFunction" → None];

SyntaxInformation[fieldLinePlot] =
  {"LocalVariables" → {"Solve", {2, 2}}, "ArgumentsPattern" → {_, _, _, OptionsPattern[]}};

SetAttributes[fieldSolve, HoldAll];
```

[2] URL:https://mathematica.stackexchange.com/questions/687/id-like-to-display-field-lines-for-a-point-charge-in-3-dimensions (accessed January 22, 2020)

As an example on how to use this code, let us look at a particular image for a $\{\frac{1}{2}, \frac{1}{2}, -\frac{1}{2}\}$ solution that was not shown in (Figure 5)

```
In[•]:= seedList =
          Flatten[Table[{{x, y, z}, 35 Pi}, {x, -1, 1, 2}, {y, -1, 1, 2}, {z, -1, 1, 2}], 2]
Out[•]= {{{-1, -1, -1}, 35 π}, {{-1, -1, 1}, 35 π}, {{-1, 1, -1}, 35 π}, {{-1, 1, 1}, 35 π},
          {{1, -1, -1}, 35 π}, {{1, -1, 1}, 35 π}, {{1, 1, -1}, 35 π}, {{1, 1, 1}, 35 π}}

In[•]:= Show[fieldLinePlot[EE[1, 0.25], {x, y, z}, seedList,
           PlotStyle → {Green, Specularity[White, 16], Tube[.03]}, PlotRange → All,
           Boxed → False, Axes → None],
         fieldLinePlot[BB[1, 0.25], {x, y, z}, seedList,
           PlotStyle → {Red, Specularity[White, 16], Tube[.03]}, PlotRange → All,
           Boxed → False, Axes → None]]
```

Out[•]=

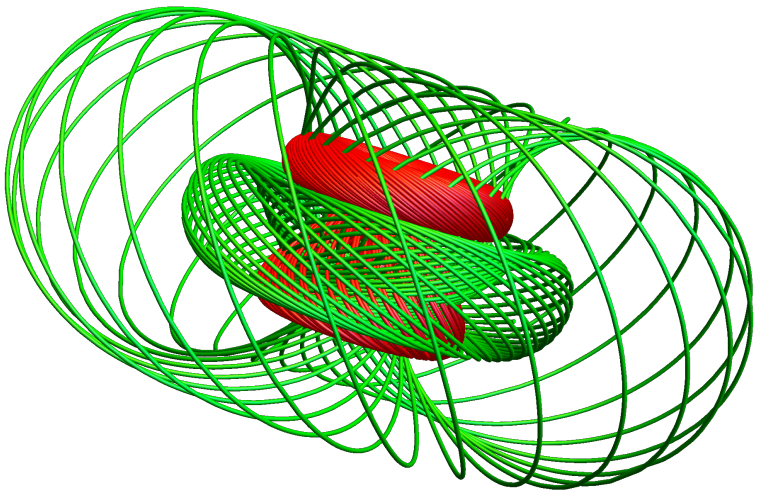

6.2.3 Routine for computing the null field condition

```
In[ ]:= Unprotect[Factorial];
Factorial[-1] := -1;
Factorial[-2] := 2;
Protect[Factorial]
Null123[J_] :=
 {f[α_] := α^(2 φ);
  g[α_, b_] := (-b / Sqrt[2])^(φ - ν) * D[f[α], {α, (φ - ν)}];
  Y[j_, m_, n_] :=
   If[j - m == 0, Sqrt[(2 j + 1) / (2 Pi^2)] * Sqrt[((2^(j - m)) * (j + m)!) / ((2 j)! * (j - m)!)] * Sqrt[((2^(j - n)) * (j + n)!) / ((2 j)! * (j - n)!)] * (g[α, b]),
    If[j - m == 1, Sqrt[(2 j + 1) / (2 Pi^2)] * Sqrt[((2^(j - m)) * (j + m)!) / ((2 j)! * (j - m)!)] * Sqrt[((2^(j - n)) * (j + n)!) / ((2 j)! * (j - n)!)] *
      (((a / (Sqrt[2]))) D[g[α, b], {b, 1}] + (-β / Sqrt[2]) D[g[α, b], {α, 1}]),
     If[j - m == 2, Sqrt[(2 j + 1) / (2 Pi^2)] * Sqrt[((2^(j - m)) * (j + m)!) / ((2 j)! * (j - m)!)] * Sqrt[((2^(j - n)) * (j + n)!) / ((2 j)! * (j - n)!)] *
       (((a / (Sqrt[2])))^2 D[g[α, b], {b, 2}] + (-β / Sqrt[2])^2 D[g[α, b], {α, 2}] - 2 (a / (Sqrt[2])) * (β / Sqrt[2]) D[D[g[α, b], α], b]),
      If[j - m == 3, Sqrt[(2 j + 1) / (2 Pi^2)] * Sqrt[((2^(j - m)) * (j + m)!) / ((2 j)! * (j - m)!)] * Sqrt[((2^(j - n)) * (j + n)!) / ((2 j)! * (j - n)!)] *
        (((a / (Sqrt[2])))^3 D[g[α, b], {b, 3}] + (-β / Sqrt[2])^3 D[g[α, b], {α, 3}] + 3 (a / (Sqrt[2])) * (β / Sqrt[2])^2 D[D[g[α, b], b], {α, 2}] -
          3 * (β / Sqrt[2]) * (a / (Sqrt[2]))^2 D[D[g[α, b], α], {b, 2}]),
       If[j - m == 4, Sqrt[(2 j + 1) / (2 Pi^2)] * Sqrt[((2^(j - m)) * (j + m)!) / ((2 j)! * (j - m)!)] * Sqrt[((2^(j - n)) * (j + n)!) / ((2 j)! * (j - n)!)] *
         (((a / (Sqrt[2])))^4 D[g[α, b], {b, 4}] + (-β / Sqrt[2])^4 D[g[α, b], {α, 4}] - 4 (a / (Sqrt[2])) * (β / Sqrt[2])^3 D[D[g[α, b], b], {α, 3}] -
           4 * (β / Sqrt[2]) * (a / (Sqrt[2]))^3 D[D[g[α, b], α], {b, 3}]), 0]]]];
  XPlusI[j_, m_, n_] := Sqrt[((j - n) * (j - n + 1)) / 2] * (Y[j, m, (n + 1)]);
  X3I[j_, m_, n_] := Sqrt[(j + 1)^2 - n^2] Y[j, m, n];
  XMinusI[j_, m_, n_] := -Sqrt[((j + n) (j + n + 1)) / 2] Y[j, m, (n - 1)];
  Z[m_, n_] := FullSimplify[{XPlusI[J, m, n] /. {φ → J, ν → (n + 1)}, XMinusI[J, m, n] /. {φ → J, ν → (n - 1)}, X3I[J, m, n] /. {φ → J, ν → n}}];
  Z123[m_, n_] := {1 / Sqrt[2] (Z[m, n][[1]] + Z[m, n][[2]]), 1 / (Sqrt[2] * I) (Z[m, n][[1]] - Z[m, n][[2]]), Z[m, n][[3]]};
  c1 := Collect[Sum[c[m, n] * Z123[m, n][[1]], {m, -J, J}, {n, -J - 1, J + 1}], {α, β, a, b}];
  c2 := Collect[Sum[c[m, n] * Z123[m, n][[2]], {m, -J, J}, {n, -J - 1, J + 1}], {α, β, a, b}];
  c3 := Collect[Sum[c[m, n] * Z123[m, n][[3]], {m, -J, J}, {n, -J - 1, J + 1}], {α, β, a, b}];
  G := c1 * c1 + c2 * c2 + c3 * c3;
  FullSimplify[Collect[G, {α, a, β, b, ab, αβ, aβ, αb}]]}
```

After obtaining the linearly independent terms from the null condition, one need to manually use them as arguments in the **Reduce**[ ] command while setting all terms individually equal to zero in order to obtain a list of possible solutions. As was mentioned before, the solution where no complex coefficient vanishes - so in a way the most general solution - then yields the quadric cone and conic equations that were discussed in chapter 4. For example, **Null123[1/2]** yields the output

$$
\begin{aligned}
&a^2\left(c\left[-\tfrac{1}{2},-\tfrac{1}{2}\right]^2-\sqrt{3}\,c\left[-\tfrac{1}{2},-\tfrac{3}{2}\right]\times c\left[-\tfrac{1}{2},\tfrac{1}{2}\right]\right)+\beta^2\left(c\left[-\tfrac{1}{2},\tfrac{1}{2}\right]^2-\sqrt{3}\,c\left[-\tfrac{1}{2},-\tfrac{1}{2}\right]\times c\left[-\tfrac{1}{2},\tfrac{3}{2}\right]\right)+\\
&b^2\left(c\left[\tfrac{1}{2},-\tfrac{1}{2}\right]^2-\sqrt{3}\,c\left[\tfrac{1}{2},-\tfrac{3}{2}\right]\times c\left[\tfrac{1}{2},\tfrac{1}{2}\right]\right)+a\,b\left(2\,c\left[-\tfrac{1}{2},-\tfrac{1}{2}\right]\times c\left[\tfrac{1}{2},-\tfrac{1}{2}\right]-\sqrt{3}\left(c\left[-\tfrac{1}{2},\tfrac{1}{2}\right]\times c\left[\tfrac{1}{2},-\tfrac{3}{2}\right]+c\left[-\tfrac{1}{2},-\tfrac{3}{2}\right]\times c\left[\tfrac{1}{2},\tfrac{1}{2}\right]\right)\right)+\\
&\beta\left(a\left(c\left[-\tfrac{1}{2},-\tfrac{1}{2}\right]\times c\left[-\tfrac{1}{2},\tfrac{1}{2}\right]-3\,c\left[-\tfrac{1}{2},-\tfrac{3}{2}\right]\times c\left[-\tfrac{1}{2},\tfrac{3}{2}\right]\right)+b\left(-3\,c\left[-\tfrac{1}{2},\tfrac{3}{2}\right]\times c\left[\tfrac{1}{2},-\tfrac{3}{2}\right]+2\,c\left[-\tfrac{1}{2},\tfrac{1}{2}\right]\times c\left[\tfrac{1}{2},-\tfrac{1}{2}\right]-c\left[-\tfrac{1}{2},-\tfrac{1}{2}\right]\times c\left[\tfrac{1}{2},\tfrac{1}{2}\right]\right)\right)+\\
&\alpha^2\left(c\left[\tfrac{1}{2},\tfrac{1}{2}\right]^2-\sqrt{3}\,c\left[\tfrac{1}{2},-\tfrac{1}{2}\right]\times c\left[\tfrac{1}{2},\tfrac{3}{2}\right]\right)+\alpha\left(a\left(c\left[-\tfrac{1}{2},\tfrac{1}{2}\right]\times c\left[\tfrac{1}{2},-\tfrac{1}{2}\right]-2\,c\left[-\tfrac{1}{2},-\tfrac{1}{2}\right]\times c\left[\tfrac{1}{2},\tfrac{1}{2}\right]+3\,c\left[-\tfrac{1}{2},-\tfrac{3}{2}\right]\times c\left[\tfrac{1}{2},\tfrac{3}{2}\right]\right)+\right.\\
&\left.\beta\left(\sqrt{3}\,c\left[-\tfrac{1}{2},\tfrac{3}{2}\right]\times c\left[\tfrac{1}{2},-\tfrac{1}{2}\right]-2\,c\left[-\tfrac{1}{2},\tfrac{1}{2}\right]\times c\left[\tfrac{1}{2},\tfrac{1}{2}\right]+\sqrt{3}\,c\left[-\tfrac{1}{2},-\tfrac{1}{2}\right]\times c\left[\tfrac{1}{2},\tfrac{3}{2}\right]\right)+b\left(-c\left[\tfrac{1}{2},-\tfrac{1}{2}\right]\times c\left[\tfrac{1}{2},\tfrac{1}{2}\right]+3\,c\left[\tfrac{1}{2},-\tfrac{3}{2}\right]\times c\left[\tfrac{1}{2},\tfrac{3}{2}\right]\right)\right)
\end{aligned}
$$

This sum contains the 10 equations expected arising from the null condition for $j=\frac{1}{2}$. The method of solving them is shown below

```
Reduce[c[-1/2, -1/2]^2 - Sqrt[3] c[-1/2, -3/2] c[-1/2, 1/2] == 0 && c[-1/2, 1/2]^2 - Sqrt[3] c[-1/2, -1/2] c[-1/2, 3/2] == 0 && c[1/2, -1/2]^2 - Sqrt[3] c[1/2, -3/2] c[1/2, 1/2] == 0 &&
 2 c[-1/2, -1/2] c[1/2, -1/2] - Sqrt[3] (c[-1/2, 1/2] c[1/2, -3/2] + c[-1/2, -3/2] c[1/2, 1/2]) == 0 && c[-1/2, -1/2] c[-1/2, 1/2] - 3 c[-1/2, -3/2] c[-1/2, 3/2] == 0 &&
 -3 c[-1/2, 3/2] c[1/2, -3/2] + 2 c[-1/2, 1/2] c[1/2, -1/2] - c[-1/2, -1/2] c[1/2, 1/2] == 0 && c[1/2, 1/2]^2 - Sqrt[3] c[1/2, -1/2] c[1/2, 3/2] == 0 &&
 c[-1/2, 1/2] c[1/2, -1/2] - 2 c[-1/2, -1/2] c[1/2, 1/2] + 3 c[-1/2, -3/2] c[1/2, 3/2] == 0 && Sqrt[3] c[-1/2, 3/2] c[1/2, -1/2] - 2 c[-1/2, 1/2] c[1/2, 1/2] + Sqrt[3] c[-1/2, -1/2] c[1/2, 3/2] == 0 &&
 -c[-1/2, -1/2] c[1/2, 1/2] + 3 c[1/2, -3/2] c[1/2, 3/2] == 0]
(c[1/2, 1/2] == 0 && c[1/2, -1/2] == 0 && c[1/2, -3/2] == 0 && c[-1/2, 1/2] == 0 && c[-1/2, -1/2] == 0 && c[-1/2, -3/2] == 0 && c[1/2, 3/2] ≠ 0) ||
 (c[1/2, 3/2] == 0 && c[1/2, 1/2] == 0 && c[1/2, -1/2] == 0 && c[-1/2, 3/2] == 0 && c[-1/2, 1/2] == 0 && c[-1/2, -1/2] == 0 && c[1/2, -3/2] ≠ 0) ||
 (c[1/2, 3/2] == 0 && c[1/2, 1/2] == 0 && c[1/2, -1/2] == 0 && c[-1/2, -3/2] == 0 && c[-1/2, 3/2] == 0 && c[1/2, 1/2] == 0 && c[-1/2, -1/2] == 0) ||
 (c[1/2, 3/2] == 0 && c[1/2, 1/2] == 0 && c[1/2, -1/2] == 0 && c[1/2, -3/2] == 0 && c[-1/2, 1/2] == 0 && c[-1/2, -1/2] == 0 && c[-1/2, -3/2] == 0 && c[-1/2, 3/2] ≠ 0) ||
 (c[1/2, 3/2] == 0 && c[1/2, 1/2] == 0 && c[1/2, -1/2] == 0 && c[1/2, -3/2] == 0 && c[-1/2, 3/2] ≠ 0 && c[-1/2, -1/2] == c[-1/2, 1/2]^2 / (Sqrt[3] c[-1/2, 3/2]) && c[-1/2, 1/2] ≠ 0 && c[1/2, -3/2] == c[-1/2, -1/2]^2 / (Sqrt[3] c[-1/2, 1/2])) ||
 (c[1/2, 3/2] ≠ 0 && c[1/2, -1/2] == c[1/2, 1/2]^2 / (Sqrt[3] c[1/2, 3/2]) && c[1/2, 1/2] ≠ 0 && c[1/2, -3/2] == c[1/2, -1/2]^2 / (Sqrt[3] c[1/2, 1/2]) && c[-1/2, 3/2] == 0 && c[-1/2, 1/2] == 0 && c[-1/2, -1/2] == 0 &&
  c[1/2, -1/2] ≠ 0 && c[-1/2, -3/2] == 0) ||
 (c[1/2, 3/2] ≠ 0 && c[1/2, -1/2] == c[1/2, 1/2]^2 / (Sqrt[3] c[1/2, 3/2]) && c[1/2, 1/2] ≠ 0 && c[1/2, -3/2] == c[1/2, -1/2]^2 / (Sqrt[3] c[1/2, 1/2]) && c[-1/2, 3/2] ≠ 0 && c[-1/2, -1/2] == 3 c[-1/2, 3/2] c[1/2, -3/2] / c[1/2, -1/2] &&
  c[-1/2, 3/2] ≠ 0 && c[-1/2, -1/2] == c[-1/2, 1/2]^2 / (Sqrt[3] c[-1/2, 3/2]) && c[1/2, 1/2] ≠ 0 && c[1/2, -3/2] == c[-1/2, -1/2]^2 / (Sqrt[3] c[-1/2, 1/2]))
```

For the general solutions (4.44), we can define a function that generates the corresponding coefficients for a value of j.

```
In[ ]:= Sol[J_] :=
  Flatten[Table[c[m, n] → Sqrt[Binomial[2 (J + 1), J + 1 - n]] * κ^((J + 1 - n) / (2 (J + 1))) * d[m],
    {m, -J, J}, {n, -J - 1, J + 1}]]
```

To test those solutions, it is simply needed to evaluate the output of **Null123**[**J**] at the values given by **Sol**[**J**]. Unfortunately, the outputs for $j = \frac{3}{2}$ and $j = 2$ are too large to be displayed in a clear form, but as the compact computation below shows, (4.44) indeed solves the null condition for those cases.

```
In[ ]:= FullSimplify[Null123[1 / 2] /. Sol[1 / 2]]
        FullSimplify[Null123[1] /. Sol[1]]
        FullSimplify[Null123[3 / 2] /. Sol[3 / 2]]
        FullSimplify[Null123[2] /. Sol[2]]

Out[ ]= {0}

Out[ ]= {0}

Out[ ]= {0}

Out[ ]= {0}
```

In order to compute the null equations for type II solutions, one has to change the definitions for X_+, X_- and X_3 in **Null123[J]** to

```
XPlusII[j_, m_, n_] := -Sqrt[((j + n) * (j + n + 1)) / 2] * (Y[j, m, (n + 1)]);
X3II[j_, m_, n_] := Sqrt[j ^ 2 - n ^ 2] Y[j, m, n];
XMinusII [j_, m_, n_] := Sqrt[((j - n) (j - n + 1)) / 2] Y[j, m, (n - 1)];
```

Acknowledgements

First I would like to thank my supervisor Prof. Dr. Olaf Lechtenfeld for his support and new ideas coming from him. I am grateful to my colleagues and friends Oscar Gawlik, Kevin Ollmann, Khairi Fahad Elyas and Yue Yu who made my time in the institute a much better one. I also want to give special thanks to Kevin Ollmann for his corrections shortly before I finished my thesis and I want to express my gratitude for my parents and my family as a whole who strongly supported me throughout my whole time studying at Leibniz university Hanover. Also I want to thank my partner Yujia Liu for making the time outside university to the most beautiful one.

References

[1] Olaf Lechtenfeld and Gleb Zhilin. A new construction of rational electromagnetic knots. *Phys. Lett.*, A382:1528–1533, 2018.

[2] Antonio F. Rañada. A topological theory of the electromagnetic field. *Letters in Mathematical Physics*, 18(2):97–106, Aug 1989.

[3] Jarosław Kopiński and José Natário. On a remarkable electromagnetic field in the Einstein Universe. *Gen. Rel. Grav.*, 49(6):81, 2017.

[4] Carlos Hoyos, Nilanjan Sircar, and Jacob Sonnenschein. New knotted solutions of Maxwell's equations. *J. Phys.*, A48(25):255204, 2015.

[5] Manuel Arrayás and Jose L. Trueba. Exchange of helicity in a knotted electromagnetic field. *Annalen Phys.*, 524:71–75, 2012.

[6] Hanno v. Bodecker and Gunnar Hornig. Link invariants of electromagnetic fields. *Phys. Rev. Lett.*, 92:030406, Jan 2004.

[7] J.L.Trueba M.Arrayás, D.Bouwmeester. Knots in electromagnetism. *Physics Reports*, Accepted 22 November 2016, Available online 30 November 2016.

[8] E. Pariat, J. E. Leake, G. Valori, M. G. Linton, F. P. Zuccarello, and K. Dalmasse. Relative magnetic helicity as a diagnostic of solar eruptivity. *Astronomy & Astrophysics*, 601:A125, May 2017.

[9] Alexei A. Pevtsov, Mitchell A. Berger, Alexander Nindos, Aimee A. Norton, and Lidia van Driel-Gesztelyi. Magnetic Helicity, Tilt, and Twist. *Space Science Reviews*, 186(1-4):285–324, Dec 2014.

[10] Keith Moffatt. Helicity and singular structures in fluid dynamics. *Proceedings of the National Academy of Sciences of the United States of America*, 111, 02 2014.

[11] William T M Irvine. Linked and knotted beams of light, conservation of helicity and the flow of null electromagnetic fields. *Journal of Physics A: Mathematical and Theoretical*, 43(38):385203, Aug 2010.

[12] Manuel Arrayás, Antonio Ranada, Alfredo Tiemblo, and Jose Luis Trueba. Null electromagnetic fields from dilatation and rotation transformations of the hopfion. *Symmetry*, 11:1105, 09 2019.

[13] Jonathan Holland and George Sparling. Null electromagnetic fields and relative cauchy-riemann embeddings. *Proceedings of the Royal Society A: Mathematical, Physical and Engineering Sciences*, 469(2152):20120583, 2013.

[14] Yoonbai Kim, Chae Young Oh, and Namil Park. Classical geometry of de sitter spacetime : An introductory review, 2002.

[15] Olaf Lechtenfeld and Gönül Ünal. Yang-mills solutions on de sitter space of any dimension. *Physical Review D*, 98(8), Oct 2018.

[16] Tatiana A. Ivanova, Olaf Lechtenfeld, and Alexander D. Popov. Finite-action solutions of Yang-Mills equations on de Sitter dS_4 and anti-de Sitter AdS_4 spaces. *JHEP*, 11:017, 2017.

[17] Ivan Cheltsov. Remarks on algebraic geometry. URL: https://www.maths.ed.ac.uk/cheltsov/gnt/notes.pdf.